Received: 20 September 2022 | Accepted: 29 December 2022

DOI: 10.1111/pce.14533

ORIGINAL ARTICLE

Plant, Cell & Environment | WILEY

Thermal optimum of photosynthesis is controlled by stomatal conductance and does not acclimate across an urban thermal gradient in six subtropical tree species

Alyssa T. Kullberg[1] | Martijn Slot[2] | Kenneth J. Feeley[1,3]

[1]Department of Biology, University of Miami, Coral Gables, Florida, USA

[2]Smithsonian Tropical Research Institute, Panama, Republic of Panama

[3]Fairchild Tropical Botanic Garden, Coral Gables, Florida, USA

Correspondence
Alyssa T. Kullberg, Department of Biology, University of Miami, 190 Cox Science Bldg, 1301 Memorial Dr, Coral Gables, FL, USA.
Email: alyssa.kullberg@gmail.com

Funding information
Tropical Fern and Exotic Plant Society

Abstract

Modelling the response of plants to climate change is limited by our incomplete understanding of the component processes of photosynthesis and their temperature responses within and among species. For ≥20 individuals, each of six common subtropical tree species occurring across steep urban thermal gradients in Miami, Florida, USA, we determined rates of net photosynthesis (A_{net}), maximum RuBP carboxylation, maximum RuBP regeneration and stomatal conductance, and modelled the optimum temperature (T_{opt}) and process rate of each parameter to address two questions: (1) Do the T_{opt} of A_{net} (T_{optA}) and the maximum A_{net} (A_{opt}) of subtropical trees reflect acclimation to elevated growth temperatures? And (2) What limits A_{net} in subtropical trees? Against expectations, we did not find significant acclimation of T_{optA}, A_{opt} or the T_{opt} of any of the underlying photosynthetic parameters to growth temperature in any of the focal species. Model selection for the single best predictor of A_{net} both across leaf temperatures and at T_{optA} revealed that the A_{net} of most trees was best predicted by stomatal conductance. Our findings are in accord with those of previous studies, especially in the tropics, that have identified stomatal conductance to be the most important factor limiting A_{net}, rather than biochemical thermal responses.

KEYWORDS
acclimation, ecophysiology, gas exchange, g_s, J_{max}, photosynthetic thermal optimum, thermal gradient, V_{cmax}

1 | INTRODUCTION

Dynamic global vegetation models and earth system models simulate the effects of future climate change on major biogeochemical cycles. These models depend on an accurate understanding of the temperature responses of the component processes of photosynthesis within and among species and across space and time (Kumarathunge et al., 2019; Lin et al., 2012). Currently, models are limited by a poor representation of the potential acclimation of the underlying components of net photosynthesis (A_{net}) to increased temperature, especially in tropical plants (Lombardozzi et al., 2015; Mercado et al., 2018; Slot et al., 2021; N. G. Smith & Dukes, 2013), due to a sparsity of empirical data characterizing temperature responses (Slot & Winter, 2017a). Earth's atmosphere has already warmed by ≥1°C since 1850–1900 and is predicted to warm by an additional 1.0–5.7°C this century, depending on emissions scenarios (IPCC, 2021). In the face of such rapid climate change, there is an imminent need to understand the global acclimation response of A_{net} to rising temperatures.

Photosynthesis has long been recognized as a temperature-sensitive process (Berry & Bjorkman, 1980; Decker, 1959; Hew et al., 1969; Mooney et al., 1978; Pearcy, 1977). A_{net} rapidly increases with leaf temperature up to a thermal optimum (T_{optA}) before rapidly decreasing again at higher leaf temperatures (Cunningham & Read, 2003; Säll & Pettersson, 1994). There is large variability in T_{optA} and in A_{net} at T_{optA} (A_{opt}) as a result of both adaptation and individual-level responses to environmental conditions, that is, acclimation (Berry & Bjorkman, 1980; Hikosaka et al., 2005; Lin et al., 2012; Way & Yamori, 2014).

Recent investigations are addressing the challenges surrounding the accurate prediction of both T_{optA} and A_{opt} acclimation responses to temperature, which stem from an incomplete understanding of the temperature responses—especially in low-latitude tropical species—of the component processes underlying variability in T_{optA} and A_{opt}, including biochemical, respiratory and stomatal processes (Dusenge & Way, 2017; Hernández et al., 2020; Kattge & Knorr, 2007; Lin et al., 2012; Rogers et al., 2017; Slot & Winter, 2017a).

The Farquhar et al. (1980) model of C3 photosynthesis expresses A_{net} in terms of its two major limiting biochemical process rates: the maximum rate of RuBP carboxylation (V_{cmax}) and the maximum rate of RuBP regeneration, or the maximum rate of electron transport (J_{max}). The Farquhar model of photosynthesis is a powerful tool for global change ecology because it mechanistically represents the effects of elevated atmospheric (CO_2) and temperature on the two major biochemical components impacting A_{net} (Medlyn et al., 2002). Across increasing leaf temperatures, both V_{cmax} and J_{max} either increase exponentially or follow a peaked Arrhenius function (Medlyn et al., 2002). Under current ambient (CO_2) and close to a given plant's T_{optA}, A_{net} is typically limited by V_{cmax} (Sage & Kubien, 2007). However, stomatal conductance (g_s), which determines the availability of CO_2 for photosynthesis and, therefore, exerts control over the achieved carboxylation and electron transport rates in C3 photosynthesis, may be of greater importance than biochemical processes in limiting A_{net}, especially in tropical (Doughty & Goulden, 2008; Hernández et al., 2020; Slot & Winter, 2017a, 2017b; Tan et al., 2017) and Mediterranean climates (Sperlich et al., 2019), and in taller, mature trees (Juárez-López et al., 2008). The temperature response of g_s follows a similar peaked temperature response to A_{net} (June et al., 2004), wherein stomata are open within a favourable temperature range, but are closed at colder temperatures and at supra-optimal temperatures associated with increased leaf-to-air vapour pressure deficit (VPD) (Peak & Mott, 2011). However, when moisture is not limiting, g_s may increase at high temperatures to regulate leaf temperatures (Feller, 2006; Reynolds-Henne et al., 2010), although decreases in A_{net} are still observed due to Rubisco inhibition (Crafts-Brandner & Salvucci, 2000; Salvucci & Crafts-Brandner, 2004) and increasing respiration in the light (Silim et al., 2010).

Major patterns of how the temperature responses of these underlying processes vary *inter*specifically across some biomes and plant functional types are relatively well understood (Crous et al., 2022; Kattge & Knorr, 2007; Kumarathunge et al., 2019), but *intra*specific responses of A_{net} and its mechanistic underpinnings to increased temperature (and increased (CO_2), and changes in water availability and humidity), that is, acclimation, remains poorly characterized, especially at low latitudes. This lack of information about intraspecific patterns can hinder the parameterization of global vegetation models (Crous et al., 2022; Kumarathunge et al., 2019) and is especially concerning considering that many tropical species may exhibit weak acclimation of A_{net} to warming (Crous et al., 2022; Dusenge, Wittemann, et al., 2021).

Multiple studies of seasonal temperature acclimation in plants have identified a decrease in the ratio of J_{max}:V_{cmax} with increasing ambient temperatures (Atkin et al., 2006; Dusenge et al., 2020; Kumarathunge et al., 2019; Lin et al., 2013; Stefanski et al., 2020). This relationship is associated with either an increase in V_{cmax} (Lin et al., 2013) or with a change in the relative amounts of relevant photosynthetic proteins associated with each process rate (Onoda et al., 2005), and may serve to counteract increased photorespiration at high temperatures (Kattge & Knorr, 2007; Kumarathunge et al., 2019; N. G. Smith & Keenan, 2020). A result of decreasing J_{max}:V_{cmax} at high temperatures is that A_{net} is less limited by RuBP carboxylation, and T_{optA} increases (Crous et al., 2022; Dusenge et al., 2020). Indeed, studies of experimentally warmed plants in temperate and boreal systems have found declines of J_{max}:V_{cmax} with increased growth temperatures of 3–4°C are associated with significant increases in T_{optA} (Hara et al., 2021; Kumarathunge et al., 2019; Sendall et al., 2015), an acclimation effect that may sometimes be sufficient to maintain A_{net} (Stefanski et al., 2020).

Similarly, experimental warming studies on tropical tree seedlings and saplings have found A_{net} to be increasingly limited by J_{max} under hotter growth temperatures (Slot & Winter, 2017c; Vårhammar et al., 2015), especially in early successional species (Slot & Winter, 2018). Furthermore, these studies have found partial to full acclimation of T_{optA} to increased growth temperatures, that is, increases in growth temperature are equal to increases in T_{optA}, but in some cases at a cost to A_{opt} (Fauset et al., 2019; Slot et al., 2021; Slot & Winter, 2017c, 2018). However, g_s may be a greater limit to A_{net} as growth temperature increases, especially when water is limiting and leaf-to-air VPD is high, as often occurs in the upper canopies of mature trees (Fauset et al., 2019). Indeed, at constant absolute humidity, VPD increases exponentially with temperature, so rising temperatures are typically accompanied by rising VPD. Finally, respiration, which typically increases exponentially with leaf temperature, has been shown to acclimate and thus may also play an important role in the overall observed acclimation of A_{net} and T_{optA} (Atkin & Tjoelker, 2003; Crous et al., 2022). More studies, especially with species from the subtropics and tropics, are needed to better characterize the long-term acclimation of photosynthetic parameters to increased growth temperatures (Dusenge & Way, 2017; Slot et al., 2021), which will improve the parameterization of global dynamic vegetation models.

Testing for the acclimation of mature trees across their development and lifetimes is logistically challenging and time consuming. 'Accidental experiments' (HilleRisLambers et al., 2013),

or pseudo-experimental setups created inadvertently by humans, can provide opportunities to address questions regarding global change while avoiding some of the challenges of true experiments. For example, urban areas are often significantly warmer than surrounding rural areas, primarily due to the prevalence of man-made surfaces that absorb solar radiation and release heat. This urban heat island effect creates thermal gradients that are exceptionally strong and steep, even over short distances within urban areas (e.g., 5°C difference over 10–100 s of metres vs. natural gradients of ~5°C per 1000 m elevation or ~5°C per 1 000 000 m latitude), making them useful settings for studying the acclimation of trees to different temperatures (Carreiro & Tripler, 2005; Esperon-Rodriguez et al., 2020; Hara et al., 2021; Kullberg & Feeley, 2022; Meineke et al., 2016; Youngsteadt et al., 2015). Other environmental factors such as CO_2, ozone and deposited nitrogen may covary with temperature on urban-to-rural gradients, but working along intra-urban temperature gradients while excluding rural areas may help to avoid significant impacts of potential confounding variables.

In this study, we compared the acclimation of photosynthetic parameters to different growth temperatures for six common tree species planted across thermal gradients in Miami, Florida, USA, urban heat island. We determined the rates of net photosynthesis (A_{net}), maximum RuBP carboxylation (V_{cmax}), maximum RuBP regeneration (J_{max}) and stomatal conductance (g_s) at a range of leaf temperatures, and modelled the thermal optimum (T_{opt}) and optimum process rate (k_{opt}) of each parameter to address two research questions: (1) Do these subtropical tree species acclimate their T_{optA} and A_{opt} to elevated growth temperatures? And (2) what limits A_{net} in these focal species, and does the limiting process vary within species based on growth temperature? We predicted that there would be consistent increases in T_{optA} and changes in A_{opt} for trees growing under hotter temperatures, but that acclimation of T_{optA} would be partial, that is, the increase in T_{optA} would be smaller than the increase in growth temperature. We also predicted species-specific changes in A_{opt} with changes in growth temperature or T_{optA}, but the directionality of this relationship should vary and be dependent on the acclimation of the various processes underlying A_{net} (Way & Yamori, 2014). Finally, we predicted that g_s would be a greater limit to the temperature response of A_{net} than the biochemical processes, and that g_s limitation would increase for trees growing in hotter areas.

2 | MATERIALS AND METHODS

This study was conducted in the urban and suburban areas of subtropical Miami-Dade County, southeast Florida, USA, taking advantage of the marked spatial variation in ambient temperatures (see below) created through the urban heat island effect. We measured gas exchange rates and estimated associated parameters on the leaves of 121 planted (i.e., not naturally recruited) trees representing six focal species (≥20 trees per species), all of which are common and widespread throughout the study area: *Bursera simaruba* (L.) Sarg., *Coccoloba uvifera* (L.) L., *Quercus virginiana* Mill., *Heptapleurum actinophyllum* (Endl.) Lowry & G.M. Plunkett, *Swietenia mahagoni* (L.) Jacq and *Terminalia catappa* L. The species *B. simaruba*, *C. uvifera*, *Q. virginiana* and *S. mahagoni* are all native to the study area, and the species *H. actinophyllum* and *T. catappa* are exotic (for more information about the study system and species, see Kullberg & Feeley, 2022).

2.1 | Sample collection

We selected focal trees to maximize the range of ambient temperatures to which they are exposed, and to capture as much of the gradient along that range as possible, rather than maximizing replication at a few select temperatures. The maximum straight-line distance between conspecific pairs was 25.2 km (Figure 1). Canopies of focal trees had near-total to total sun exposure, and no samples were collected close to tall buildings or structures that could shade the trees. Between June and October 2021, we collected a roughly 1 m long (±0.3 m) sun-exposed branch from the outer canopy of each tree between 08:00 and 09:30 local time (for *H. actinophyllum* we collected individual leaves due to them having thick branches and sufficient petiole length to maintain water transport). We immediately placed the cut branch ends into water and covered the branches and leaves with opaque plastic bags to maintain a dark, humid environment and to prevent wilting. We recorded the percent of ground cover that was impervious to water (i.e., concrete or pavement) within a 5 m radius of each tree and collected two soil cores (up to 15 cm deep when bedrock was deep enough) within 3 m of each tree; soil cores were subsequently mixed to create one aggregate soil sample per tree. Soil samples were air-dried in the laboratory for at least 1 week before analyses.

Upon returning to the laboratory (within 1 h of sample collection), branches were re-cut under water to promote water transport, re-covered with plastic to prevent wilting, and allowed to acclimate to the laboratory conditions for >1 h before connecting to the gas analyser. Connected branches were left to acclimate to ambient air/light and preset leaf chamber conditions for at least 30 min before data collection. While it is generally preferable to measure gas exchange on leaves of attached branches, this is not always possible for sun-exposed canopy branches of adult trees. Some previous studies have shown no significant effects of branch excision on photosynthetic parameters (Verryckt et al., 2020), while other studies (Davidson et al., 2022) have shown that afternoon stomatal conductance measurements may be reduced for excised branches in some species—in particular, in latex-producing species the maximum rates of A_{net}, V_{cmax} and J_{max} may be significantly reduced in excised branches (Santiago & Mulkey, 2003). Since we did not use any latex-produce species in our study and since we are primarily interested in within-species relationships, we expect that our results were not significantly affected by branch excision.

2.2 | Gas exchange measurements

To estimate the thermal optima (T_{opt}) and the temperature responses of the underlying biochemical mechanisms limiting net photosynthesis

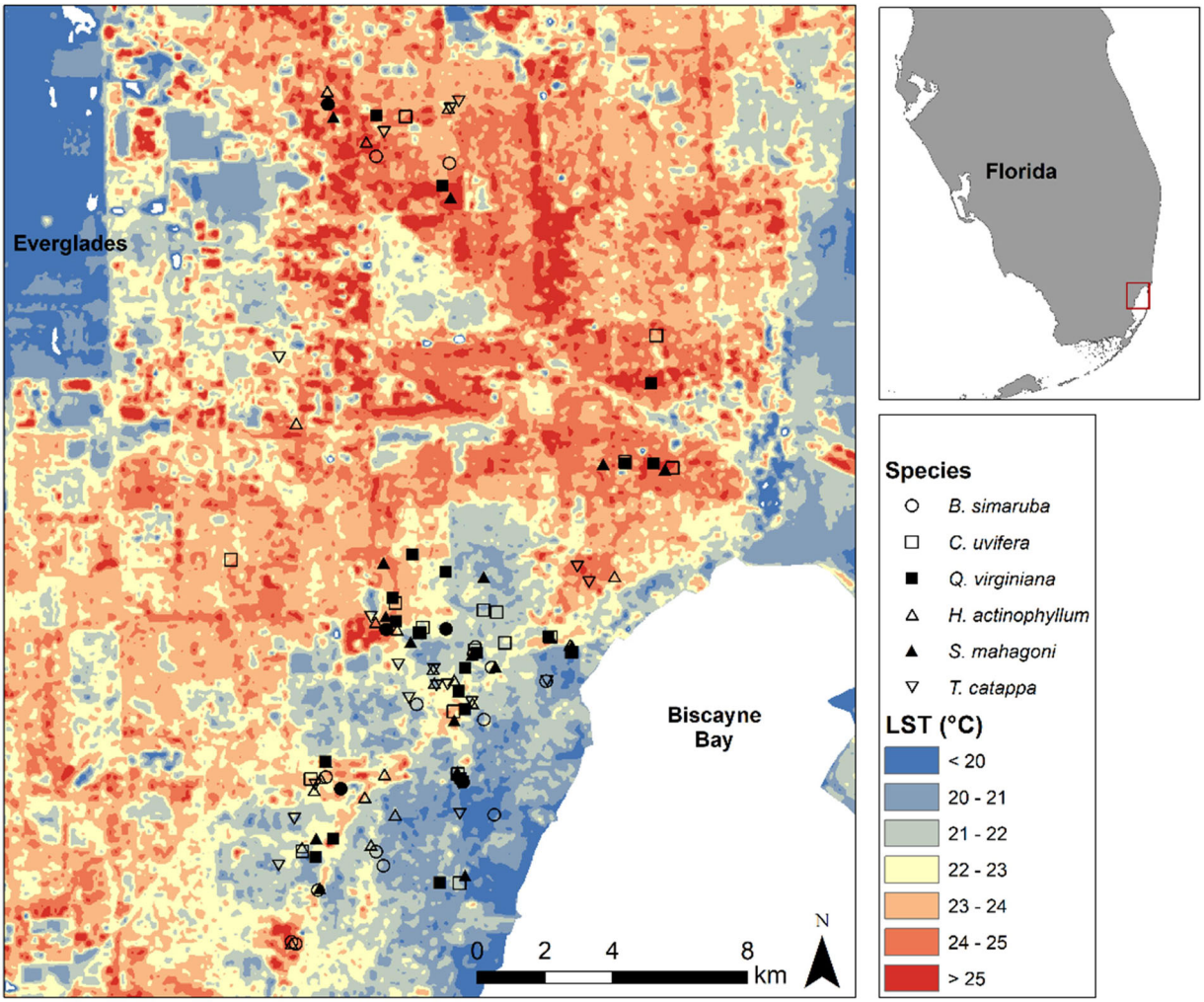

FIGURE 1 A map of the study area in the Miami urban heat island, showing land surface temperature (LST) and the location of each focal tree

(A_{net}) of individual trees, we measured net CO_2 assimilation across a range of leaf intercellular CO_2 concentrations (AC_i curves) nested within a range of leaf temperatures. Specifically, we measured gas exchange rates at 12 different ambient CO_2 concentrations ranging from 50 to 2000 ppm nested within 10 different leaf temperatures (24°C, 26°C, 28°C, 30°C, 32°C, 34°C, 36°C, 38°C, 40°C and 42°C) using a LiCor LI-6800 portable gas exchange system (LI-COR Inc.). All gas exchange measurements were conducted in a laboratory setting, and all environmental conditions were manipulated only inside the leaf chamber using an LI-6800. The gas exchange rates were measured on one healthy, mature leaf per focal individual (resulting in 120 measurements per tree), which were clamped into the 6 cm^2 aperture leaf chamber if leaf lamina were large enough and otherwise were clamped into the 2 cm^2 aperture leaf chamber. Reference CO_2 concentrations and leaf temperatures were controlled by the LI-6800 instrument for all measurements, leaf surface irradiance was maintained at 1000 µmol quanta m^{-2} s^{-1}, and the sample VPD was set to 1.5 kPa (to prevent condensation within the LI-6800 at lower temperatures). Keeping a constant VPD avoids confounding changes in temperature with changes in VPD on stomatal conductance (g_s), especially at high temperatures where stomatal aperture may be independent of A_{net} (Urban et al., 2017). To avoid sensor drift, the LI-6800's reference and sample chamber infra-red gas analysers were matched before each measurement. We programmed stability criteria for the instrument to determine when it was appropriate to log a measurement, including the slope of A_{net} (slope limit of 0.8 and SD of 1 over 15 s) and g_s (slope limit of 0.2 and SD of 1 over 15 s). We had the instrument wait at least 2 min between measurements to reach stability (and an additional 4 min when changing leaf temperature) and allowed up to 3 min before logging measurements. In total, it took approximately 4.5 h per leaf to conduct the gas exchange measurements at all 12 reference CO_2 concentrations at all 10 leaf temperatures, and the same leaf remained within the leaf chamber during the entire protocol.

2.3 | Parameter estimation and temperature responses

We estimated the maximum rate of Rubisco carboxylation (V_{cmax}) and the maximum rate of electron transport for RuBP regeneration (J_{max})

with the 'fitaci' function in the 'plantecophys' package (Duursma, 2015) in R (v. 4.1.2) after visually inspecting the data for each AC_i curve and omitting any measurements that fell outside a reasonable range of values (0 ppm < C_i < 2500 ppm and −1 µmol CO_2 m^{-2} s^{-1} < A_{net} < 50 µmol CO_2 m^{-2} s^{-1}) or varied greatly from an otherwise visually discernible curve, a sign of the LI-6800 not reaching stability before logging a measurement. Unfortunately, the first point taken for the AC_i curves (at ambient [CO_2] (C_a) = 400 ppm) were often discarded since extra time was generally required to reach stability after a change in leaf temperature. We estimated V_{cmax} and J_{max} for each measured leaf temperature instead of using the default correction to 25°C. We inspected every modelled AC_i curve visually and omitted curves with less than 5 points.

To estimate the T_{opt} of V_{cmax} (T_{optV}) and J_{max} (T_{optJ}) for each individual, we fit the following peaked Arrhenius equation with the 'nls' function in *R* according to Medlyn et al. (2002):

$$f(T_{leaf}) = k_{opt} \frac{H_d \times e^{\left(\frac{H_a(T_{leaf}-T_{opt})}{T_{leaf}\times R\times T_{opt}}\right)}}{H_d - H_a\left(1 - e^{\left(\frac{H_d(T_{leaf}-T_{opt})}{T_{leaf}\times R\times T_{opt}}\right)}\right)}, \quad (1)$$

where T_{leaf} is leaf temperature (in *K*), k_{opt} is the process rate of either V_{cmax} (V_{opt}) or J_{max} (J_{opt}) at the respective T_{opt} (in µmol m^{-2} s^{-1}) of each; H_a is the activation energy of the Arrhenius function or the exponential rise before T_{opt}; *R* is the universal gas constant (0.008314 kJ K^{-1} mol^{-1}); and H_d is the deactivation energy, or the decrease after T_{opt}, fixed at 400 kJ mol^{-1} to avoid overparameterization of the models. We set H_d to 400 kJ mol^{-1} after determining that it explained on average, a greater proportion of variance in the temperature response of both V_{cmax} and J_{max} than the more standard 200 kJ mol^{-1} (Medlyn et al., 2002) in most of our study species (Supporting Information: Figure S1; setting H_d to 400 kJ mol^{-1} tended to allow the model to better approximate the high observed maximum process rates of V_{cmax} and J_{max}).

Starting values for estimating parameters were set as H_a = 100 kJ mol^{-1}, k_{opt} = the maximum value of either V_{cmax} or J_{max} and T_{opt} = the leaf temperature corresponding to the maximum value of either V_{cmax} or J_{max}. We estimated V_{cmax25} and J_{max25} as the fitted peaked Arrhenius model predictions of each process rate at 25°C to evaluate if J_{max25}:V_{cmax25} (i.e., the ratio between these two processes) decreased with increasing growth temperature as observed in previous studies (Kattge & Knorr, 2007; Kumarathunge et al., 2019; N. G. Smith & Dukes, 2013). We also estimated the ratio of J_{max} and V_{cmax} at T_{optA} ($J_{maxTopt}$:$V_{cmaxTopt}$). Additionally, we calculated the entropy term (Δ*S*) of V_{cmax} and J_{max} according to Medlyn et al. (2002) and Slot et al. (2021) as:

$$\Delta S = \frac{H_d}{T_{opt}} + R \quad \ln\left(\frac{H_a}{H_d - H_a}\right). \quad (2)$$

We examined the temperature response of the activation state of Rubisco following the methods of Sage et al. (2008), wherein the slope of the linear regression of observed A_{net} values at low C_i (≤200 ppm, where Rubisco activase should not be limited by ATP supply) may be compared to the initial slope of the modelled AC_i curve, which follows the assumption that Rubisco is fully activated:

$$\text{Initial slope} = \frac{V_{cmax}}{\left(\Gamma^* + K_C\left(1 + \frac{O}{K_O}\right)\right)}, \quad (3)$$

where Γ* is the CO_2 compensation point in the absence of dark respiration and K_C and K_O are the Michaelis–Menten constants for CO_2 and O_2, respectively, which are both temperature-dependent parameters calculated per treatment temperature according to Bernacchi et al. (2001). O is the concentration of O_2 in the chloroplast stroma, assumed to be 210 mbar. By comparing the observed initial slope against the modelled slope at low C_i where electron transport is not limiting, we tested the model's assumption that Rubisco is fully activated at a given leaf treatment temperature.

The temperature response of observed versus modelled Rubisco activation was then modelled by fitting generalized additive models (GAMs) with the 'mgcv' package (Wood, 2017) in R, using cubic regression splines fit with restricted maximum likelihood, as in Slot et al. (2021). Rubisco activation was determined to be significantly reduced where 1.96 times the standard error of the observed and modelled GAMs did not overlap.

A_{net} and g_s were modelled as functions of temperature following the model presented in June et al. (2004):

$$k(T_{leaf}) = k_{opt} \times e^{-\left(\frac{T_{leaf}-T_{opt}}{\Omega}\right)^2}, \quad (4)$$

where T_{leaf} is leaf temperature, k_{opt} is the process rate of either assimilation (A_{opt}) or g_s (g_{opt}), and Ω is defined as the difference between the temperatures above and below T_{opt} at which the process rate is reduced by ~37% from k_{opt}. Since many measurements of A_{net} had to be discarded when C_a was set to 400 ppm due to insufficient acclimation time to new T_{leaf}, A_{net} was extracted from each AC_i curve as the net C assimilation rate modelled at the respective intercellular CO_2 concentration (C_i, in ppm) measured when C_a was set to 400 ppm. While our reported A_{net} values are, therefore, estimations based on modelled AC_i curves, this method allowed us to integrate all the collected photosynthesis data into the estimates of A_{net}. g_s was calculated as the average measured g_s when C_i was ±150 ppm of the C_i of extracted A_{net}.

Stomatal limitation (*l*) was determined according to (Farquhar & Sharkey, 1982), Slot and Winter (2017b), and Hernández et al. (2020) as:

$$l = 1 - \frac{A_{obs}}{A_{infg_s}}, \quad (5)$$

where A_{obs} is the observed rate of A_{net} and $A_{inf\ gs}$ is the rate of A_{net} if there were no stomatal limitation, determined according to the Farquhar et al. (1980) model of C3 photosynthesis as:

$$V_{cmax} = \frac{A_g(C_i + K_c)}{C_i - \Gamma^*}, \quad (6)$$

where C_i is set to C_a (around 400 ppm) and A_g is the rate of light-saturated photosynthesis plus respiration in the light (estimated as $0.015 \times V_{cmax}$). $A_{inf\ gs}$ was then determined as A_g minus respiration in the light.

2.4 | Growth temperatures

We estimated the relative ambient temperature at the location of each focal tree based on the land surface temperature (LST) measured with remotely sensed imagery. To create a map of LST, we used a Landsat 8 (Level-1, Collection-1) image taken on 5 January 2021, at 15:50, downloaded from the United States Geological Survey (USGS) EarthExplorer (Landsat Missions). This was the clearest image over the study area for the year before sample collection based on a filter to only include images in the search with <40% cloud cover and visual inspection of images. The Landsat 8 thermal band has 100-m resolution, but LST is calculated at 30-m resolution due to a correction for emissivity based 30-m resolution data on normalized difference vegetation index (NDVI). We calculated LST following USGS protocol (Jeevalakshmi et al., 2017; Kullberg & Feeley, 2022). We then determined the LST at each tree location using the 'extract' function of the 'raster' package in R. In a previous publication, we showed that Landsat 8-derived LST in Miami are highly correlated ($r \geq 0.8$) across months (October to May) and years (2016–2021), indicating that the relative temperature patterns in Miami are consistent across time and seasons, although the absolute temperatures may vary (Kullberg & Feeley, 2022).

2.5 | Soil parameters

We measured the pH of each soil sample (one aggregate sample per tree location) using an Extech ExStik II pH/conductivity probe. Samples were prepared by mixing 10 g of dried, crushed soil with 10 ml deionized water, which was then allowed to rest for 30 min before inserting the pH probe into the sample and waiting for the reading to stabilize. The pH probe was calibrated before each use with buffer solutions of pH 4, 7 and 10. For soil nitrogen (N), phosphorus (P) and potassium (K), we used the LaMotte NPK Soil Kit (3-5880) and followed standardized protocols to categorize nutrient concentrations into six categories: trace, trace/low, low, low/medium, medium, medium/high, or high.

2.6 | Hypothesis testing

To test our first hypothesis that subtropical trees have a limited ability to acclimate their T_{optA} and A_{opt} to elevated temperatures across thermal gradients, we constructed linear least squares regressions comparing the T_{optA} and the A_{opt} of each focal individual to LST or % impervious cover. We further explored potential relationships between underlying biochemical and physiological processes to environmental factors and photosynthetic optima. We tested for relationships between the T_{opt}s and k_{opt}s of V_{cmax}, J_{max} or g_s and LST, % impervious cover, T_{optA} or A_{opt}. We also examined relationships for $J_{maxTopt}$:$V_{cmaxTopt}$, J_{max25}:V_{cmax25}, and the slopes of J_{max}:V_{cmax} or I over leaf temperature, compared to LST, % impervious cover, T_{optA} or A_{opt}.

To address the possibility that the acclimation responses of T_{optA} and A_{opt} covary with environmental factors other than temperature, we constructed linear mixed models (LMMs) using the 'lmerTest' package in R (Kuznetsova et al., 2017). We set the full models with the response variable as either T_{optA} or A_{opt}, species as a random intercept and the environmental factors of LST, % impervious cover (as a rough proxy for water availability), soil soluble N, P and K, and soil pH as fixed effects. Next, we used the 'step' function to perform backward stepwise model selection given the full model and without reducing random effects (i.e., species effects).

To further explore which parameter (V_{cmax}, J_{max} or g_s) is most limiting to A_{net}, we used the 'leaps' package in R (Lumley, 2004) to search exhaustively for the best single-predictor model of A_{net} for each tree using a branch-and-bound algorithm and using R^2, adjusted R^2 and Mallows' C_p as selection criteria (Slot & Winter, 2017a). We repeated this algorithm twice per individual, once using the assimilation at all leaf temperatures tested, and again using just the leaf temperatures that are greater than T_{optA} of that individual. While this model selection method does not directly account for mechanistic dynamics between g_s, V_{cmax} and J_{max} across temperature, it allowed us to compare the overall limitations to photosynthesis across leaf temperatures with the high-temperature limitations to photosynthesis.

Once we identified the single best predictor of A_{net} for each tree, we tested whether the difference in the best predictor between the individuals of a given species was associated with differences in either T_{optA} or the R^2 of the predictive model using analysis of variance (ANOVA). Finally, we compared the proportion of individuals per species that were best predicted by each variable using ANOVA, to see if there was a single variable that consistently predicted A_{net} across species.

3 | RESULTS

Gas exchange measurements on the 121 individuals across 10 leaf measurement temperatures per tree resulted in 1152 successfully modelled AC_i curves. A summary of the linear relationships between the temperature responses of different photosynthesis parameters to growth temperature and % impervious cover and to each other can be found in Supporting Information: Tables S1 and S2, respectively.

3.1 | k_{opt}—T_{opt} relationships by species

A_{opt} was significantly positively correlated with T_{optA} in one of the study species, *H. actinophyllum* (Figure 2), although this species had

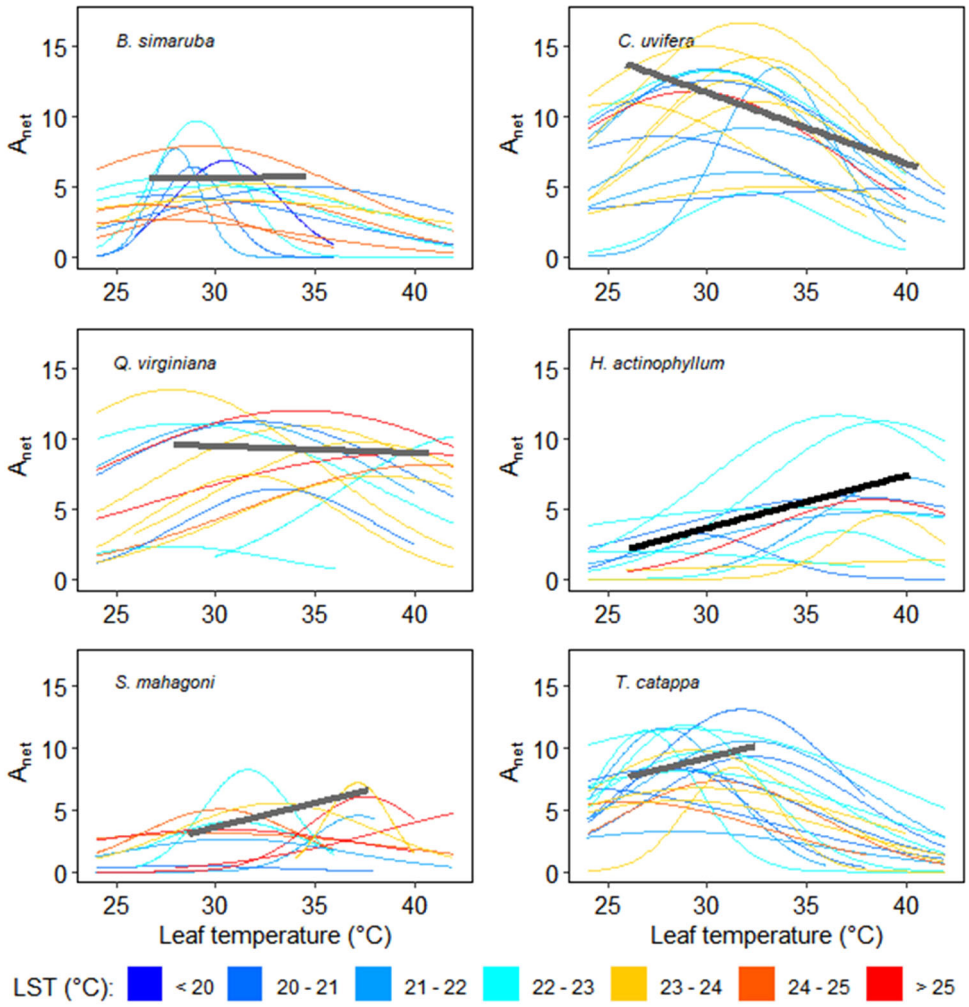

FIGURE 2 Modelled temperature response curves of A_{net} (μmol CO_2 m^{-2} s^{-1}), where each panel is a separate study species, and each curve is one tree. Curves were modelled with the 'nls' package in R using Equation 4. The colour of each curve indicates the relative growth temperature of the tree based on land surface temperature (LST). Black and grey straight lines represent the significant and nonsignificant, respectively, linear regressions of the optimum rate of photosynthesis (A_{opt}) over the thermal optimum of photosynthesis (T_{optA}). The distribution of pseudo-R^2 values for the 'nls' models is reported by species in Supporting Information: Figure S3.

the greatest variability in the goodness of fit of its modelled A_{net} temperature response curves (Supporting Information: Figure S3). Indeed, the goodness-of-fit of the temperature response curves of both A_{net} and g_s were highly variable across individuals of most species (Supporting Information: Figures S3 and S6). V_{opt} was significantly positively correlated with T_{optV} in *B. simaruba* ($p = 0.03$, adj. $R^2 = 0.30$) and *Q. virginiana* ($p = 0.002$, adj. $R^2 = 0.44$; Figure 3), the two study species with the greatest goodness of fit of their V_{cmax} temperature response curves (Supporting Information: Figure S4). Also, the activation energy of V_{cmax} (H_{aV}) was negatively related to T_{optV} in four species, including *B. simaruba* ($p = 0.001$, adj. $R^2 = 0.48$), *C. uvifera* ($p < 0.001$, adj. $R^2 = 0.51$), *H. actinophyllum* ($p = 0.03$, adj. $R^2 = 0.17$) and *T. catappa* ($p = 0.002$, adj. $R^2 = 0.41$; Supporting Information: Figure S7A); and H_{aV} was positively related to V_{opt} in *T. catappa* ($p = 0.001$, adj. $R^2 = 0.44$; Supporting Information: Figure S7B). J_{opt} was significantly positively related to T_{optJ} in *C. uvifera* ($p = 0.03$, adj. $R^2 = 0.23$; Figure 3). The activation energy of J_{max} (H_{aJ}) was negatively related to T_{optJ} in three species: *B. simaruba* ($p = 0.045$, adj. $R^2 = 0.18$), *C. uvifera* ($p = 0.007$, adj. $R^2 = 0.34$) and *T. catappa* ($p = 0.04$, adj. $R^2 = 0.19$; Supporting Information: Figure S7C), and H_{aJ} was positively related to T_{optJ} in *S. mahagoni* ($p = 0.03$, adj. $R^2 = 0.22$; Supporting Information: Figure S7C). H_{aJ} was positively related to J_{opt} for one species, *T. catappa* ($p = 0.002$, adj. $R^2 = 0.42$; Supporting Information: Figure S7D). g_{opt} was significantly positively related to T_{optg} in *Q. virginiana* ($p = 0.01$, adj. $R^2 = 0.37$) and *S. mahagoni* ($p = 0.003$, adj. $R^2 = 0.41$; Figure 3).

In most trees, the activation state of Rubisco did not limit A_{net} at any temperature—observed slopes were not significantly reduced relative to modelled slopes, and the fitted curves overlapped (ANOVA and Tukey's HSD, $p < 0.001$ between frequency of individuals with complete overlap and frequency of all other categories of curve noncoincidence; Figure 4). However, 10%–25%

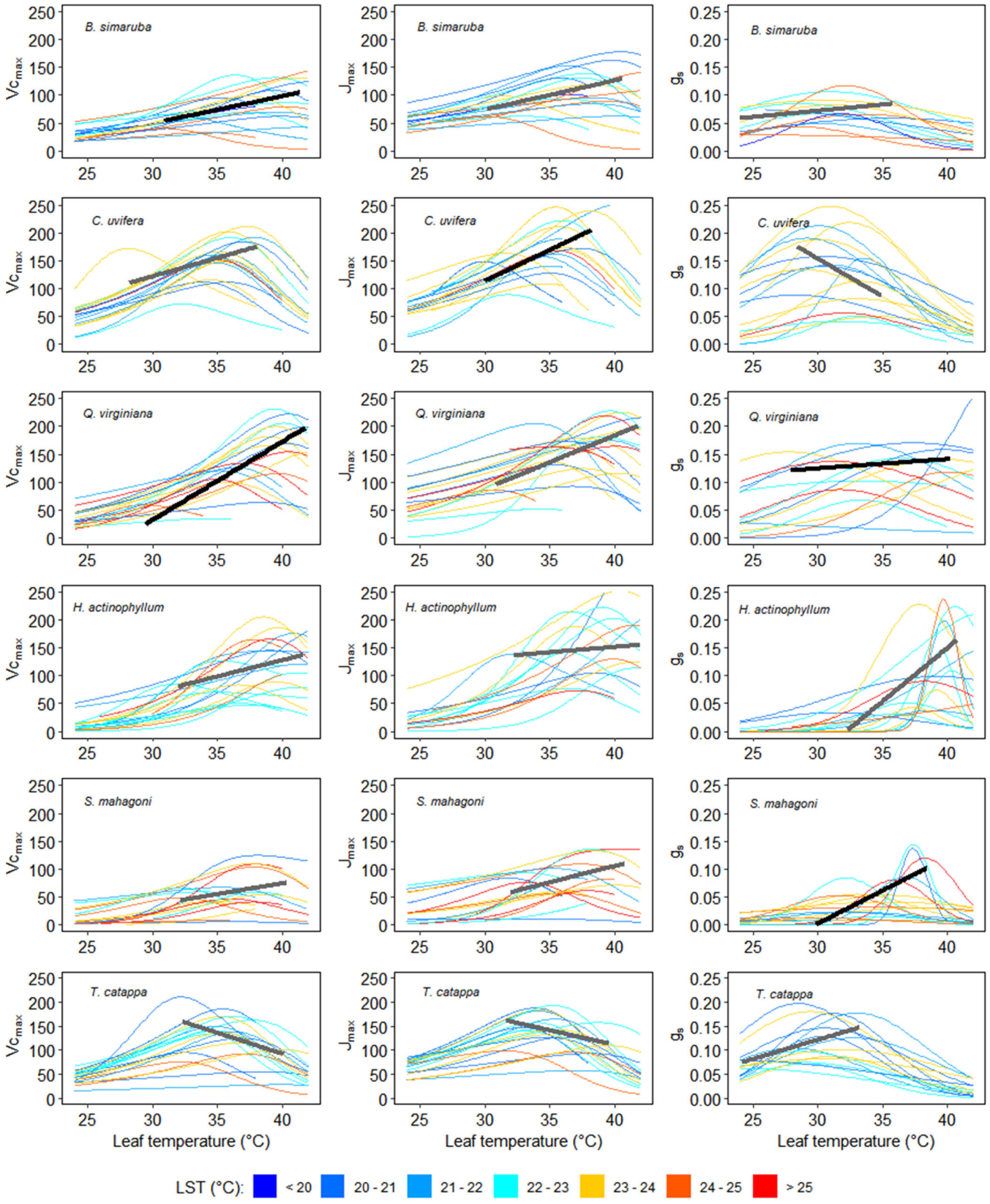

FIGURE 3 Modelled temperature response curves of V_{cmax} and J_{max} (μmol m^{-2} s^{-1}) (Equation 1) and of g_s (mol m^{-2} s^{-1}) (Equation 2). Each row of plots is a single study species, and within each panel, each curve is one tree. The colour of each curve indicates the relative growth temperature based on land surface temperature (LST). Black and grey straight lines represent the significant and nonsignificant, respectively, linear regressions of the optimum process rate (k_{opt}) over the thermal optimum of the given process (T_{optk}). The distribution of pseudo-R^2 values for the 'nls' models is reported by parameter and species in Supporting Information: Figures S4–S6.

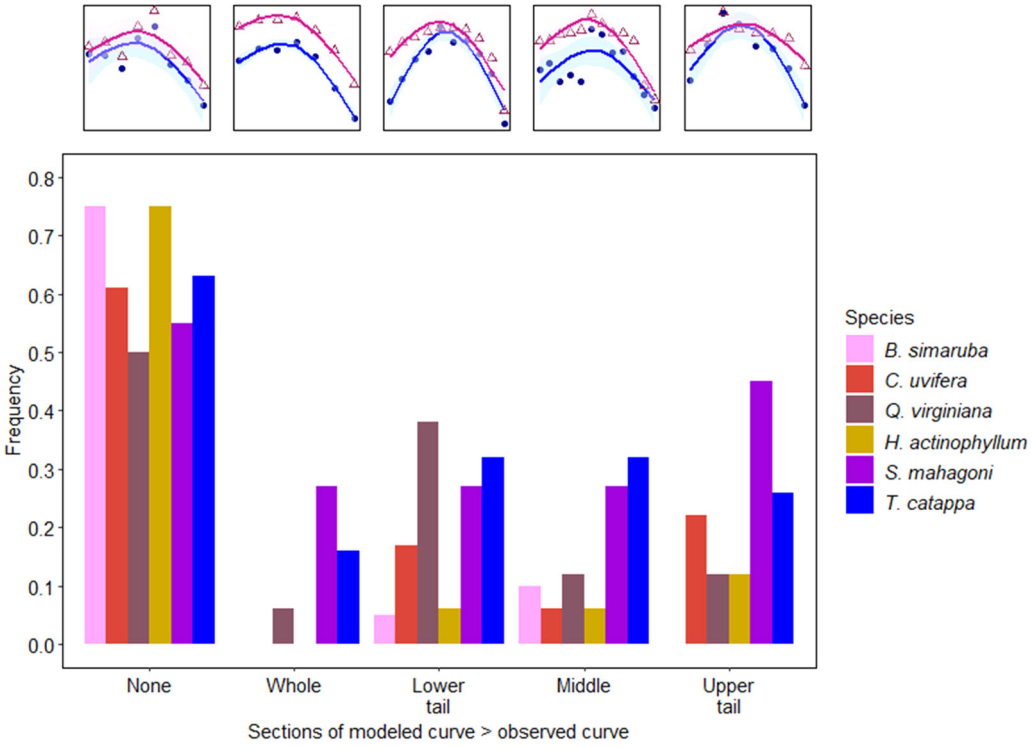

FIGURE 4 The sections of the temperature response curve of Rubisco activation that are significantly greater when calculated based on the modelled initial slope of the AC_i curve (i.e., using V_{cmax}) than when calculated based on the observed initial slope of the AC_i curve (i.e., using raw data points at $C_i < 200$ ppm). The top panels show exemplar figures of each category of curve noncoincidence; the modelled curve of each individual is red, the observed curve is blue, and the shaded regions are the standard error of the generalized additive model. In the main bottom panel, curve noncoincidence is summarized by individual and grouped by species.

of individuals in all species except *B. simaruba* did have reduced Rubisco activation at high treatment temperatures. *Q. virginiana* and *T. catappa* also had reduced Rubisco activation at relatively low temperatures in 30%–40% of individuals.

3.2 | T_{opt} and k_{opt} relationships to growth temperature (LST) and other environmental factors

Against expectations, T_{optA} did not have a significant positive relationship to LST in any of the six study species (Figure 5a). Similarly, no species showed a significant relationship between A_{opt} and LST (Figure 5b). There were also no significant single-species relationships between either T_{optA} or A_{opt} and % impervious cover (Figure 5c,d).

Similarly, there were also almost no significant single-species relationships between LST and any of the other photosynthesis variables of interest (T_{optV}, V_{opt}, T_{optJ}, J_{opt}, T_{optg}, J_{max}:V_{cmax}, J_{max25}:V_{cmax25}, $J_{maxTopt}$:$V_{cmaxTopt}$, g_{opt}, *l*), the one exception being a significant negative relationship between T_{optV} and LST and between T_{optJ} and LST for *Q. virginiana* (Supporting Information: Table S5). Additionally, none of the species showed notable relationships between % impervious cover and the photosynthesis variables (Supporting Information: Table S5).

When all environmental variables were used to construct a stepwise LMM predicting T_{optA}, soil soluble phosphorus (P) and potassium (K) were the only predictors selected for the final model ($p = 0.004$ and $p = 0.054$, respectively; Table S2). However, this relationship can be attributed almost entirely to between-species relationships and not to intraspecific relationships (marginal $R^2 = 0.09$, conditional $R^2 = 0.50$). Moreover, in single-species analysis, P had only a marginally significant positive relationship with T_{optA} in three of the study species, *B. simaruba* ($p = 0.06$), *Q. virginiana* (0.07), and *H. actinophyllum* (0.09). *K* was not significantly related to T_{optA} for any single-species analysis.

3.3 | Relationships between underlying photosynthetic processes and T_{optA} and A_{opt}

A_{opt} correlated positively with V_{opt}, J_{opt} and g_{opt} for most species (Figure 6d,h,l, Supporting Information: Table S3), but exhibited no relationships with the T_{opt} of these parameters (Figure 6b,f,j). T_{optA} consistently correlated with T_{optg} in all species (Figure 6i, Supporting Information: Table S4), and for some species T_{optA} correlated with the temperature optima or optimum rates of V_{cmax}, J_{max} or g_s (Figure 6a,c,e,g,k).

The slope of J_{max}:V_{cmax} over measurement leaf temperatures was significantly negatively correlated with T_{optA} for *Q. virginiana* (Figure 7a, Supporting Information: Table S4) and significantly positively correlated with A_{opt} for *C. uvifera* (Figure 7b, Supporting

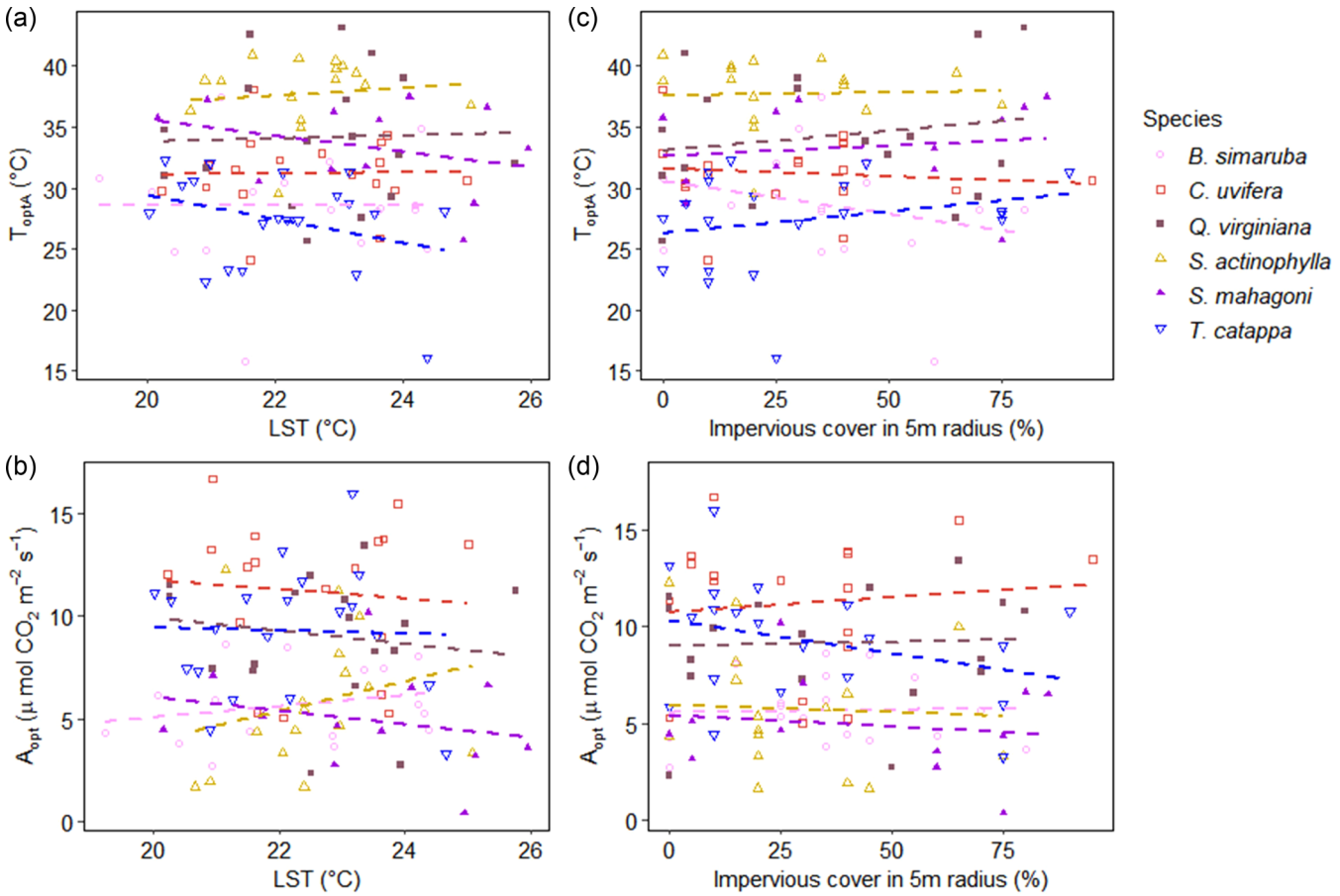

FIGURE 5 Within-species linear least squares relationships between land surface temperature (LST) and (a) the thermal optimum of net photosynthesis (T_{optA}) and (b) the rate of photosynthesis at its thermal optimum (A_{opt}), and between percent impervious cover within 5 m of each tree and (c) T_{optA} and (d) A_{opt} (all nonsignificant, $p > 0.05$). Each point is a single tree.

Information: Figure S3). J_{max25}:V_{cmax25} was not related to T_{optA} in any species (Figure 7c, Supporting Information: Table S4) and was significantly negatively associated with A_{opt} in *B. simaruba* and *T. catappa* (Figure 7d, Supporting Information: Figure S3). $J_{maxTopt}$:$V_{cmaxTopt}$ showed a significant negative association with T_{optA} for *B. simaruba* and *S. mahagoni* (Figure 7e, Supporting Information: Figure S4). $J_{maxTopt}$:$V_{cmaxTopt}$ also showed a significant negative relationship with A_{opt} for *B. simaruba*, *S. mahagoni* and *T. catappa* (Figure 7f, Supporting Information: Figure S3).

The slope of stomatal limitation (l) over leaf temperature decreased significantly with increased T_{optA} (Figure 7g, Supporting Information: Figure S4) for one species, *Q. virginiana*. In other words, trees of *Q. virginiana* with higher T_{optA} were less limited by stomatal conductance when leaf temperatures are high, which is consistent with the observation that g_s and A_{net} of *Q. virginiana* are comparatively high, even at 40°C. l showed a significant negative association with A_{opt} in one species, *H. heptapleurum* (Figure 7h, Supporting Information: Figure S3).

Finally, the individuals of our study species for which the activation state of Rubisco was significantly reduced at the upper end of the temperature response curve (Figure 4—upper tail) did not show a significant association to reduced A_{opt}.

3.4 | Limiting factor of A_{net}

There were no clear patterns regarding relationships between T_{optA} and the best predictor of A_{net} for any of the six study species when using a branch-and-bound algorithm to model A_{net} (Figure 8a). There were also no major patterns regarding the R^2 of the single-predictor model of A_{net} and the predictor of the model (i.e., models predicted by any given variable were not necessarily stronger than those predicted by other variables), except for *T. catappa*, which had significantly higher R^2 for models predicted by g_s compared to those predicted by either J_{max} ($p = 0.04$) or V_{cmax} ($p = 0.002$) (Figure 8b). Interestingly, *T. catappa* was also the only species to show a significant LMM relationship between the R^2 of the single-predictor model and T_{optA} with the model predictor as a random intercept ($p = 0.007$, marginal $R^2 = 0.21$, conditional $R^2 = 0.57$, Supporting Information: Figure S2).

The A_{net} of most individuals across all six study species was limited by g_s. The relative frequency of individuals for which g_s is the single best predictor of A_{net} across treatment temperatures (0.73, averaged across species) is significantly greater than the frequency of individuals limited by either J_{max} (mean = 0.09, $p < 0.0001$) or V_{cmax} (mean = 0.18, $p < 0.0001$) (Figure 8c). The single best predictor of A_{net}

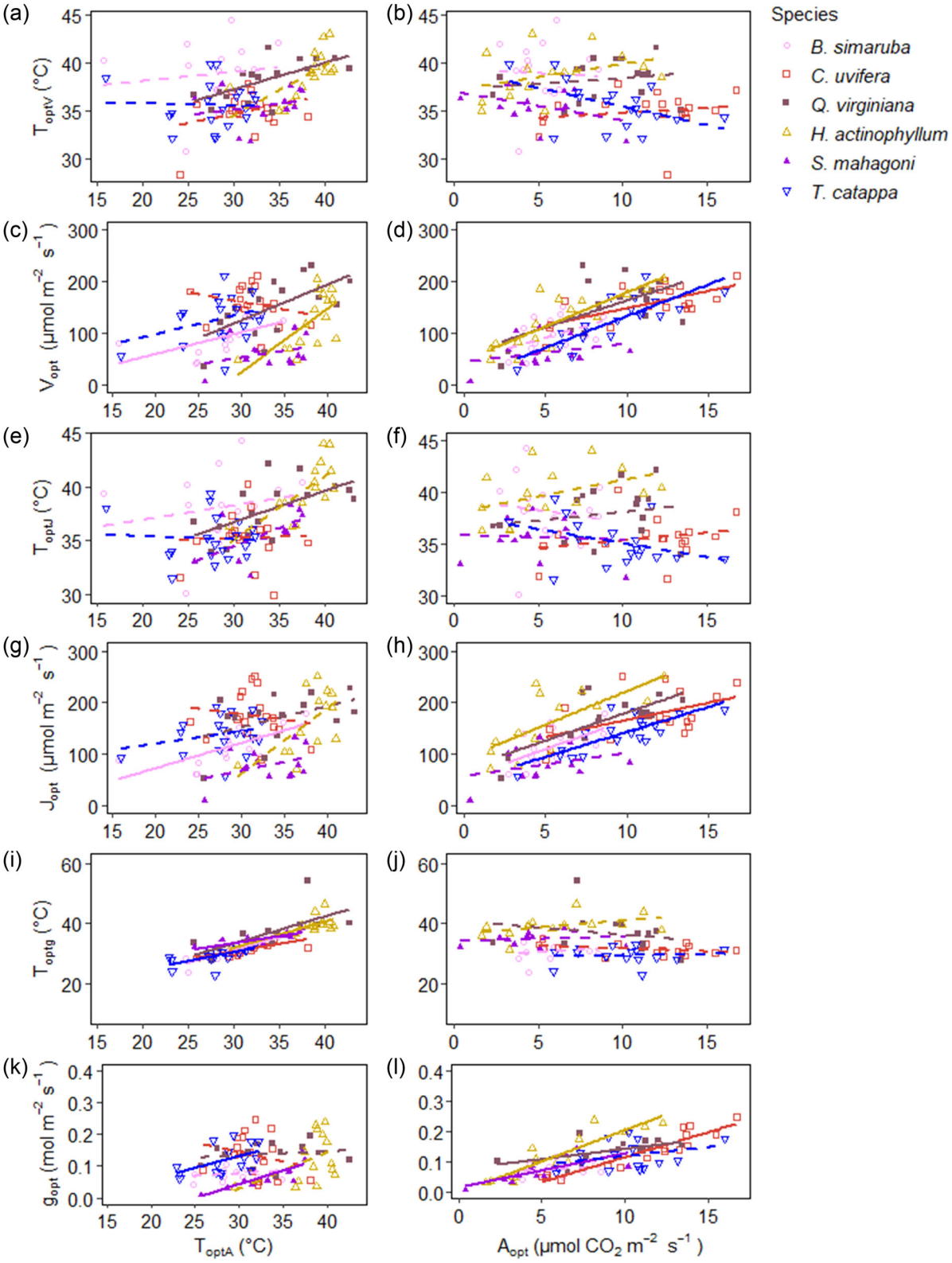

FIGURE 6 Within-species relationships for the thermal optima (T_{opt}s) and optimum process rates (k_{opt}s) of the underlying factors affecting net photosynthesis (A_{net}) over T_{optA} (optimum temperature of net photosynthesis, left (a, c, e, g, i, k) and A_{opt} (net photosynthetic rate at the optimum temperature, right (b, d, f, h, j, l). Each point represents an individual tree, solid lines are significant relationships ($p < 0.05$), and dotted lines are nonsignificant relationships.

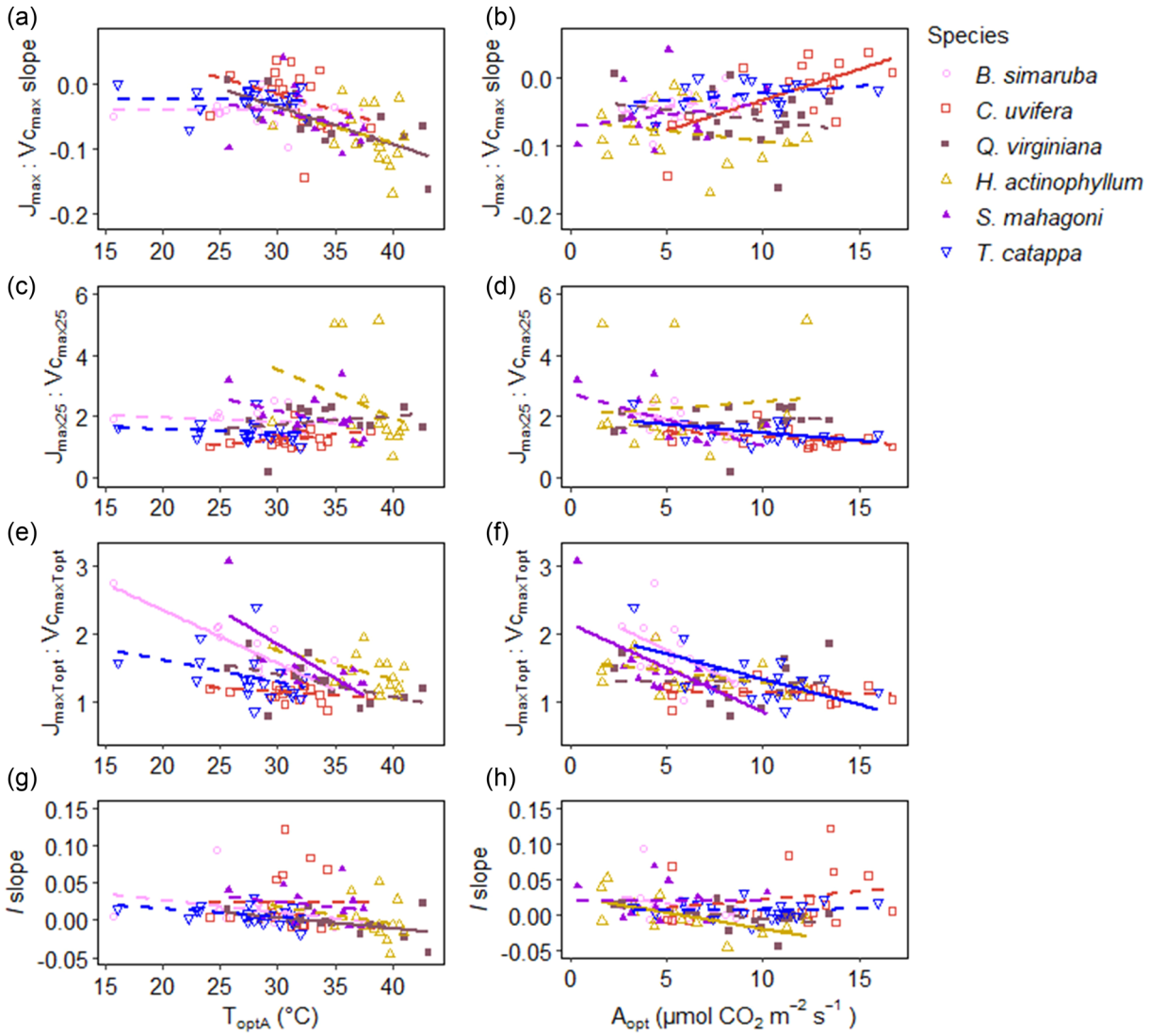

FIGURE 7 Within-species relationships for T_{optA} (optimum temperature of net photosynthesis, left) and A_{opt} (net photosynthetic rate at the optimum temperature, right) explained by (a, b) the slope of J_{max}:V_{cmax} over leaf measurement temperatures (T_{leaf}); (c, d) $J_{maxTopt}$:$V_{cmaxTopt}$; (e, f) J_{max25}:V_{cmax25} and (g, h) the slope of the relationship between stomatal limitation (I) (Equations 3 and 4) and T_{leaf}. Each point represents an individual tree, solid lines are significant relationships ($p < 0.05$), and dotted lines are nonsignificant relationships.

at high temperatures (above T_{optA}) was the same as when using data from all leaf temperatures in most individuals (77%), and there was no clear pattern for when the best predictor was different between the full model and the high-temperature model.

4 | DISCUSSION

4.1 | Photosynthetic thermal optima do not acclimate to different growth temperatures

Contrary to our a priori predictions, the six subtropical tree species that we studied did not acclimate their thermal optima of net photosynthesis (T_{optA}) to temperature differences across the Miami urban heat island. Likewise, although the goodness-of-fit of the models estimating T_{optA} and g_s were highly variable between individuals, there was little evidence for thermal acclimation for any of the underlying photosynthetic parameters. Notably, against expectations (Crous et al., 2018; Perez et al., 2021), this lack of thermal acclimation did not correspond to significant changes in maximum net photosynthesis rates (A_{opt}) at high growth temperatures. Taken together, these results indicate that growth temperature differences of up to 5°C did not induce thermal acclimation in any of our study species and did not lead to differences in maximum photosynthetic performance.

Our results are similar to those of Dusenge, Wittemann, et al. (2021), who found no evidence of T_{optA} acclimation in their study of two tropical montane tree species. However, there is a substantial body of literature that has found significant acclimation of T_{optA} to increased growth temperatures (Crous et al., 2022;

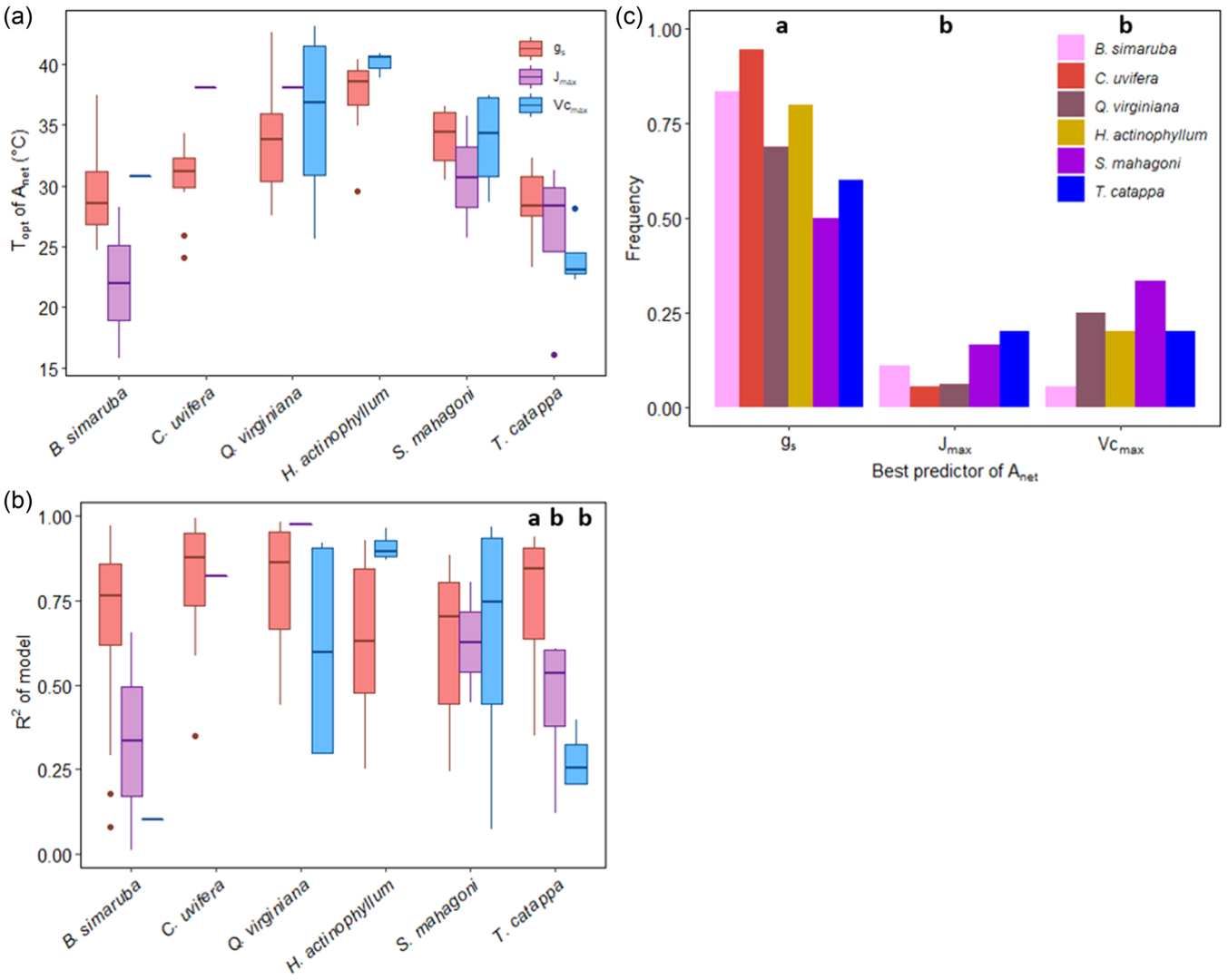

FIGURE 8 (a) The thermal optimum of net photosynthesis (T_{optA}) by the photosynthesis component that best predicted A_{net} for each tree in a single-predictor branch-and-bound algorithm model, separated by study species. (b) R^2 of the single-predictor model of A_{net} for each tree by the predictor of that model, separated by study species. (c) The relative frequencies of the component of photosynthesis most strongly predicting A_{net}. Each coloured bar represents individuals of a different species. Letters indicate significant differences between groups (one-way analysis of variance).

Hall et al., 2013; Kumarathunge et al., 2019; Way & Sage, 2008; Yamaguchi et al., 2016), even in tropical tree species (Slot et al., 2021). Contrary to our results, previous studies have also shown decreasing A_{opt} with increasing T_{optA} due to performance tradeoffs in the underlying processes (Berry & Bjorkman, 1980; Dusenge, Wittemann, et al., 2021; Slot et al., 2021; Way & Sage, 2008), although in a meta-analysis Way and Yamori (2014) demonstrated that acclimation of T_{optA} does not correspond to a consistent response in A_{opt} across 103 species, possibly related to a cross-biome pattern of reduced ability to acclimate towards the tropics (Crous, 2019; Crous et al., 2018).

Although our satellite-derived measures of LST likely provide an accurate characterization of between-site variability in relative growth temperature (Bechtel, 2011; Connors et al., 2013; Estoque & Murayama, 2017; Kullberg & Feeley, 2022), they may not adequately account for the microclimate conditions of the sample material (Conry et al., 2014; Gluch et al., 2006). Temperatures can vary over spatial scales smaller than 30 m (the resolution of Landsat 8 satellite images), meaning that individual trees or leaves may be acclimated to microclimate conditions that vary considerably from the larger-scale site conditions (Carter et al., 2021). However, an effect of microsite conditions on photosynthetic temperature responses is not always observed (Hernández et al., 2020). In addition, variations of other environmental variables like CO_2 and ozone may obscure a potential temperature effect, although we believe that such effects should be minimized in our study by sampling only within urban Miami and excluding rural or natural areas.

Also, each tree in our study was represented by measurements from a single leaf, which increases the potential for introducing variation that can obscure patterns. To counter this limitation, we only sampled fully sun-exposed leaves, and we sampled trees across a large range of LSTs (maximum of ~6°C between sites) to buffer against the potential effects of microsite differences.

T_{optA} should acclimate based on leaf temperatures rather than air temperatures (Knoerr & Gay, 1965; Wright et al., 2017). We only sampled fully sun-exposed leaves, and by standardizing the radiation load across sites, patterns in leaf temperatures should follow patterns in LST (our measure of growth temperature) if the trees have sufficient access to water. Nonetheless, acclimation of thermoregulatory traits that impact leaf energy balance, such as leaf area, thickness, spectral properties and stomatal properties, may obscure acclimation of photosynthesis by decoupling leaf temperatures and air temperatures. However, in a previous study, we did not find evidence of strong thermal trait acclimation in these same tree species and urban heat island systems (Kullberg & Feeley, 2022). With recent advances in technology such as drones equipped with thermal cameras, it may be possible to measure in situ canopy leaf temperatures more accurately. Going forward, it will be crucial to utilize these emerging technologies to help characterize the temperature dynamics of urban trees and their physiological responses to climate.

Another possibility for the observed lack of acclimation of T_{optA} to growth temperatures is uncertainty in parameter estimation. The parameterization of our A_{net} temperature response curves relied on ≤10 data points to estimate three parameters in a four-parameter non-linear least squares model. The low number of data points compared to estimated parameters meant that the goodness of fit of the A_{net} temperature response curves was sometimes low. Inaccurate parameter estimates of T_{optA} and A_{opt} may obscure relationships with growth temperature.

Finally, the observed lack of T_{optA} acclimation across growth temperatures may have been due to adaptational differences between individuals of varying seed sources. The trees we sampled were of various ages and size classes and were located across various municipalities in Miami Dade County, so we anticipate that possible that the sample trees of any given species were most likely from multiple seed sources. However, seed source information was not available for the trees in our study, so we are unable to determine the extent of this potential source of error. Future studies could potentially isolate the effects of acclimation and local adaptation by incorporating information on population genetics.

4.2 | Urban heat islands provide a potential window into future climate change effects

Despite the fact that we did not observe the acclimation of photosynthetic parameters to growth temperature, we emphasize the potential utility of the urban heat islands as 'accidental experiments' to test the potential effect of future climate change on trees and other species (Bussotti et al., 2014; Carreiro & Tripler, 2005; Cregg & Dix, 2001; Farrell et al., 2015). Urban heat islands provide steep thermal gradients with levels of warming on par with predicted climate change for this century and often have planted (i.e., not naturally dispersed) trees that facilitate the separation between adaptive and acclimatory effects—something that is not typically possible in observational studies along large-scale elevation or latitudinal gradients.

4.3 | Thermal optima of V_{cmax} and J_{max} have moderate control over the thermal optima of A_{net}

Growth temperature and other environmental variables did not significantly impact A_{net} within any of our study species. Of all the environmental variables included in this study (LST, impervious cover, soil pH, N, P and K), soil soluble P and K were the only variables that were related to T_{optA} according to stepwise LMM analysis. Most of the variability explained by soil P and K, however, was attributable to between-species differences rather than intraspecific variation. Accordingly, for our subsequent analyses, we explored the acclimation of the component processes underlying A_{net}, irrespective of abiotic conditions. We found various significant single-species relationships between T_{optA} or A_{opt} and the T_{opt} of some of the individual component processes as well as with their respective optimum process rates (k_{opt}), highlighting the processes that drive T_{optA} and A_{opt}. Importantly, however, we did not directly measure respiration in the light in this study and were, therefore, unable to determine the relative influence of acclimation of respiration compared to other underlying processes of A_{net} on the acclimation of T_{optA} and A_{opt}.

We found that the T_{opt} of both V_{cmax} and J_{max} were somewhat positively related to T_{optA} (observed in two and three species, respectively) and therefore appear to have a moderate role in driving differences in T_{optA} across species. This result is consistent with previous studies that have found that these two biochemical thermal responses generally relate to shifts in T_{optA} (Crous et al., 2022; Hikosaka et al., 2005; Medlyn et al., 2002; Onoda et al., 2005). In most of our study species (all except for *S. mahagoni*), any observed increase in T_{optV} and T_{optJ} with T_{optA} was not due to increased activation energies, H_{aV} and H_{aJ} (Dusenge, Wittemann, et al., 2021; Kattge & Knorr, 2007). However, Hikosaka et al. (2005) found H_{aV} to be the most important factor allowing the acclimation of T_{optA}.

Increased T_{optA} was related to decreased entropy terms (ΔS) of the temperature responses of V_{cmax} and J_{max} in just one species, *H. actinophyllum*, providing only limited support that these intraspecific relationships in our study reflect previous intra- and interspecific findings that the negative temperature response of ΔS is more or less generalized across species (Kattge & Knorr, 2007; Slot et al., 2021). In addition, the activation state of Rubisco in most trees across all the study species did not significantly limit A_{net}, and individuals in which Rubisco limitation was observed at high temperatures did not have significantly reduced A_{opt}. This result is

similar to some observations on the tropical tree *Tabebuia rosea* (Slot et al., 2021) and various herbaceous species (Sage et al., 2008), but contrary to other results showing significant high-temperature Rubisco deactivation in herbaceous species (Haldimann & Feller, 2005; Yamori et al., 2006) and the boreal tree *Picea mariana* (Sage et al., 2008).

Upregulation of both V_{opt} and J_{opt} in most species (four and five species, respectively) was associated with an increase in A_{opt}, as expected (Crous et al., 2022). Although the thermal optima of V_{cmax} and J_{max} play a relatively moderate role in regulating T_{optA}, the greater the rates of these processes at their respective T_{opt}s (V_{opt} and J_{opt}) still led to significantly increased A_{opt}.

Finally, $J_{maxTopt}$:$V_{cmaxTopt}$ was lower when plants had a higher T_{optA}. This pattern of decreasing J_{max}:V_{cmax} with increasing T_{optA} has been found previously (Crous et al., 2022; Dusenge et al., 2020; Hikosaka et al., 2005; Kumarathunge et al., 2019) and is an acclimation response associated with higher growth temperatures, typically associated with raising V_{cmax} relative to J_{max} to relieve the carboxylation limitation often observed at high temperatures. Although a clear pattern with growth temperature was not evident in the current study, we did find a significant negative relationship between $J_{maxTopt}$:$V_{cmaxTopt}$ and T_{optA} in some species. In other words, when a tree is performing at a relatively low T_{optA}, J_{max} and V_{cmax} operate relatively lower on their own temperature response curves, where J_{max} is proportionally greater compared to V_{cmax} than when the process rates operate closer to their respective thermal optima at higher temperatures. The J_{max}:V_{cmax} ratio at T_{optA} can thus vary with T_{optA} without shifts in the temperature response curves of J_{max} and V_{cmax}, and since T_{optA} was more strongly forced by g_s than by the two biochemical processes, this appears to explain the pattern observed in our study.

4.4 | A_{net} is most strongly limited by g_s across leaf temperatures

We found multiple lines of evidence suggesting that g_s is the primary component affecting A_{net}. While V_{cmax} and J_{max} have strong effects on A_{net} at a given stomatal conductance, T_{optA} and T_{optg} are typically lower than T_{optV} and T_{optJ}. Thus, between T_{optA} and T_{optV} or T_{optJ}, A_{net} decreases with temperature despite the fact that V_{cmax} and J_{max} are still increasing—this strongly suggests that at those temperatures, A_{net} is primarily limited by stomatal conductance to CO_2. Furthermore, T_{optA} in all six study species was significantly positively related to T_{optg} despite considerable variability in the goodness of fit of these two temperature response curves in most species, indicating that the temperature response of A_{net} is significantly driven by the temperature response of g_s. However, for trees with higher T_{optA}, the positive association between T_{optA} and T_{optg} was only associated with reduced stomatal limitation (l) at high leaf temperatures (i.e., closer to T_{optA}) for one species, *Q. virginiana*. In other words, although T_{optA} is highly dependent on T_{optg}, trees with a higher T_{optA} do not necessarily benefit from reduced stomatal limitation when performing at their T_{optA}, although visually there is a weakly decreasing trend in the slope values of l over increasing leaf treatment temperatures with increasing T_{optA}, as was expected. Interestingly, *Q. virginiana* is at the southernmost end of its range in Miami, whereas the other five study species are at their northern range limits, indicating that the plasticity of stomatal limitation may depend on a species' latitude of origin. Like J_{max} and V_{cmax}, g_{opt} was also positively related to A_{opt} in four of the study species and showed relatively higher R^2 values than the two biochemical process rates, indicating that the rate of g_s plays a significant role in limiting A_{opt}.

Because V_{opt}, J_{opt} and g_{opt} were all significantly positively correlated with A_{opt} in most of our study species, it was difficult to determine the overall relative impact of these three processes on A_{net}. To address this uncertainty, we conducted the single-predictor model selection analysis to determine which of the three processes was the best predictor of A_{net} across leaf treatment temperatures for each tree. We found that g_s was the single best predictor of A_{net} in most trees, which was true across all six species. Out of the six species, *S. mahagoni* had proportionally the fewest individuals in which A_{net} was best predicted by g_s, likely because g_s tended to remain very low across leaf measurement temperatures in this species. The best predictor of A_{net} was not related to whether the full set of leaf treatment temperatures was included or only those >T_{optA}, to the R^2 of the model, or to the T_{optA} of the tree, so we could not determine a reason for the differences in the best predictor between trees of the same species. *T. catappa* was the only exception as the one species to show a significant positive relationship between the R^2 of the single-predictor model and the T_{optA}. Therefore, for *T. catappa*, individuals with higher T_{optA} are more strongly limited by a single predictor, and furthermore that predictor is most likely to be g_s.

There is a growing number of studies on the limitations of A_{net}, especially in tropical species, that support our finding that stomatal conductance is of great importance (Carter et al., 2021; Grossiord et al., 2020; Rowland et al., 2015; Slot & Winter, 2016, 2017a; M. N. Smith et al., 2020; Tan et al., 2017; Wong et al., 1979). This general finding is in contrast to observations from temperate systems where photosynthesis appears to be more strongly controlled by V_{cmax} (Sage & Kubien, 2007; Scafaro et al., 2017; Yamaguchi et al., 2016), especially at high temperatures (Hikosaka et al., 2005; Way & Sage, 2008), and is sometimes limited by J_{max} (Sage & Kubien, 2007). There is, however, recent evidence that even some higher-latitude trees may face stomatal limitation to A_{net} at elevated temperatures, although the response appears to be species-specific (Dusenge, Ward, et al., 2021).

As the general importance of stomatal conductance in limiting A_{net} becomes clearer, it is necessary to determine how the confounding effects of temperature and water limitation act to alter rates of stomatal conductance and, in turn, affect A_{net} (Tan et al., 2017). For example, elevated leaf-to-air VPD, which tends to increase with increased temperatures and decreasing water availability, often causes stomatal closure (Lin et al., 2012). This is especially true in sun versus shade leaves (Hernández et al., 2020) and in tropical versus temperate species (Cunningham, 2004), possibly because of a tropical-to-temperate isohydry-anisohydry

gradient (Meinzer et al., 2017). Moreover, current models suggest that tropical forests are currently operating beyond their thermal and VPD optima (Rowland et al., 2015), so parsing out the specific effects of temperature versus water stress on stomatal conductance is of great importance.

5 | CONCLUSION

We did not detect evidence of acclimation of photosynthesis to elevated growth temperatures within adults of six subtropical tree species growing across a range of temperatures in Miami's urban heat island. However, we also did not observe a decline in A_{opt} at increased growth temperatures, so while there is no evidence for T_{optA} acclimation, there is no indication that heat island temperatures are limiting the photosynthetic performance of our study species. These results are contrary to the findings of previous studies that have identified limited acclimation of the thermal optimum of net photosynthesis (T_{optA}), occasionally at a cost to the rate of net photosynthesis at its thermal optimum (A_{opt}). We found evidence that all three underlying photosynthetic components included in our study —V_{cmax}, J_{max} and stomatal conductance—have varying levels of control on T_{optA} as well as A_{opt}, confirming that they are each at least partially responsible for determining the overall temperature response of A_{net}. However, the study species differed greatly in terms of correlations among photosynthetic parameters, emphasizing the potential for highly species-specific responses to environment, which complicates the prediction of future tree performance. We also found that A_{net} was most often limited by stomatal conductance in all six species. This suggests that the controls on A_{net} in the subtropics are more like those in the tropics than in temperate zones and highlights the need for continued investigation of the environmental controls to stomatal conductance.

ACKNOWLEDGEMENTS

The authors would like to acknowledge H. Alwahadneh and C. Elliott for their assistance in data collection. A.T.K. also thanks the Tropical Fern and Exotic Plant Society for awarding a scholarship that made possible the field work for this study.

DATA AVAILABILITY STATEMENT

The data that support the findings of this study are available from the corresponding author upon reasonable request.

ORCID

Alyssa T. Kullberg http://orcid.org/0000-0002-1521-439X
Martijn Slot http://orcid.org/0000-0002-5558-1792

REFERENCES

Atkin, O.K., Scheurwater, I. & Pons, T.L. (2006) High thermal acclimation potential of both photosynthesis and respiration in two lowland Plantago species in contrast to an alpine congeneric. *Global Change Biology*, 12, 500–515.

Atkin, O.K. & Tjoelker, M.G. (2003) Thermal acclimation and the dynamic response of plant respiration to temperature. *Trends in Plant Science*, 8, 343–351.

Bechtel, B. (2011) Multitemporal Landsat data for urban heat island assessment and classification of local climate zones. In: Stilla, U., Gamba, P., Juergens, C. &Maktav, D. (Eds.) *2011 Joint Urban Remote Sensing Event*. Institute of Electrical and Electronics Engineers, pp. 129–132.

Bernacchi, C.J., Singsaas, E.L., Pimentel, C., Portis Jr, A.R. & Long, S.P (2001) Improved temperature response functions for models of Rubisco-limited photosynthesis. *Plant, Cell & Environment*, 24, 253–259.

Berry, J. & Bjorkman, O. (1980) Photosynthetic response and adaptation to temperature in higher plants. *Annual Review of Plant Physiology*, 31, 491–543.

Bussotti, F., Pollastrini, M., Killi, D., Ferrini, F. & Fini, A. (2014) Ecophysiology of urban trees in a perspective of climate change. *Agrochimica*, 58, 247–268.

Carreiro, M.M. & Tripler, C.E. (2005) Forest remnants along urban-rural gradients: examining their potential for global change research. *Ecosystems*, 8, 568–582.

Carter, K.R., Wood, T.E., Reed, S.C., Butts, K.M. & Cavaleri, M.A. (2021) Experimental warming across a tropical forest canopy height gradient reveals minimal photosynthetic and respiratory acclimation. *Plant, Cell & Environment*, 44, 2879–2897.

Connors, J.P., Galletti, C.S. & Chow, W.T.L. (2013) Landscape configuration and urban heat island effects: assessing the relationship between landscape characteristics and land surface temperature in Phoenix, Arizona. *Landscape Ecology*, 28, 271–283.

Conry, P., Fernando, H.J.S., Leo, L.S., Sharma, A., Potosnak, M. & Hellmann, J. (2014) Multi-Scale Simulations of Climate-Change Influence on Chicago Heat Island. *Chicago: American Society of Mechanical Engineers 2014 4th Joint US-European Fluids Engineering Division Summer Meeting collocated with the American Society of Mechanical Engineers 2014 12th International Conference on Nanochannels, Microchannels, and Minichannels*.

Crafts-Brandner, S.J. & Salvucci, M.E. (2000) Rubisco activase constrains the photosynthetic potential of leaves at high temperature and CO2. *Proceedings of the National Academy of Sciences*, 97, 13430–13435.

Cregg, B.M. & Dix, M.E. (2001) Tree moisture stress and insect damage in urban areas in relation to heat island effects. *Journal of Arboriculture*, 27, 8–17.

Crous, K.Y. (2019) Plant responses to climate warming: physiological adjustments and implications for plant functioning in a future, warmer world. *American Journal of Botany*, 106, 1049–1051.

Crous, K.Y., Drake, J.E., Aspinwall, M.J., Sharwood, R.E., Tjoelker, M.G. & Ghannoum, O. (2018) Photosynthetic capacity and leaf nitrogen decline along a controlled climate gradient in provenances of two widely distributed Eucalyptus species. *Global Change Biology*, 24, 4626–4644.

Crous, K.Y., Uddling, J. & De Kauwe, M.G. (2022) Temperature responses of photosynthesis and respiration in evergreen trees from boreal to tropical latitudes. *New Phytologist*, 234, 353–374.

Cunningham, S.C. (2004) Stomatal sensitivity to vapour pressure deficit of temperate and tropical evergreen rainforest trees of Australia. *Trees*, 18, 399–407.

Cunningham, S.C. & Read, J. (2003) Do temperate rainforest trees have a greater ability to acclimate to changing temperatures than tropical rainforest trees? *New Phytologist*, 157, 55–64.

Davidson, K.J., Lamour, J., Rogers, A. & Serbin, S.P. (2022) Late-day measurement of excised branches results in uncertainty in the estimation of two stomatal parameters derived from response curves in *Populus deltoides* bartr. × *Populus nigra* L. *Tree Physiology*, 42, 1377–1395.

Decker, J.P. (1959) Comparative responses of carbon dioxide outburst and uptake in tobacco. *Plant Physiology*, 34, 100–102.

Doughty, C.E. & Goulden, M.L. (2008) Are tropical forests near a high temperature threshold? *Journal of Geophysical Research: Biogeosciences*, 113, G00B07.

Dusenge, M.E., Madhavji, S. & Way, D.A. (2020) Contrasting acclimation responses to elevated CO_2 and warming between an evergreen and a deciduous boreal conifer. *Global Change Biology*, 26, 3639–3657.

Dusenge, M.E., Ward, E.J., Warren, J.M., Stinziano, J.R., Wullschleger, S.D. & Hanson, P.J. et al. (2021) Warming induces divergent stomatal dynamics in co-occurring boreal trees. *Global Change Biology*, 27, 3079–3094.

Dusenge, M.E. & Way, D.A. (2017) Warming puts the squeeze on photosynthesis–lessons from tropical trees. *Journal of Experimental Botany*, 68, 2073–2077.

Dusenge, M.E., Wittemann, M., Mujawamariya, M., Ntawuhiganayo, E.B., Zibera, E., Ntirugulirwa, B. et al. (2021) Limited thermal acclimation of photosynthesis in tropical montane tree species. *Global Change Biology*, 27, 4860–4878.

Duursma, R.A. (2015) Plantecophys-an R package for analysing and modelling leaf gas exchange data. *PLoS One*, 10, e0143346.

Esperon-Rodriguez, M., Rymer, P.D., Power, S.A., Challis, A., Marchin, R.M. & Tjoelker, M.G. (2020) Functional adaptations and trait plasticity of urban trees along a climatic gradient. *Urban Forestry & Urban Greening*, 54, 126771.

Estoque, R.C. & Murayama, Y. (2017) Monitoring surface urban heat island formation in a tropical mountain city using Landsat data (1987–2015). *ISPRS Journal of Photogrammetry and Remote Sensing*, 133, 18–29.

Farquhar, G.D., von Caemmerer, S. & Berry, J.A. (1980) A biochemical model of photosynthetic CO_2 assimilation in leaves of C_3 species. *Planta*, 149, 78–90.

Farquhar, G.D. & Sharkey, T.D. (1982) Stomatal conductance and photosynthesis. *Annual Review of Plant Physiology*, 33, 317–345.

Farrell, C., Szota, C. & Arndt, S.K. (2015) Urban plantings: 'living laboratories' for climate change response. *Trends in Plant Science*, 20, 597–599.

Fauset, S., Oliveira, L., Buckeridge, M.S., Foyer, C.H., Galbraith, D. & Tiwari, R. et al. (2019) Contrasting responses of stomatal conductance and photosynthetic capacity to warming and elevated CO_2 in the tropical tree species *Alchornea glandulosa* under heatwave conditions. *Environmental and Experimental Botany*, 158, 28–39.

Feller, U. (2006) Stomatal opening at elevated temperature: an underestimated regulatory mechanism. *General Applied Plant Physiology*, 32, 19–31.

Gluch, R., Quattrochi, D.A. & Luvall, J.C. (2006) A multi-scale approach to urban thermal analysis. *Remote Sensing of Environment*, 104, 123–132.

Grossiord, C., Buckley, T.N., Cernusak, L.A., Novick, K.A., Poulter, B., Siegwolf, R.T.W. et al. (2020) Plant responses to rising vapor pressure deficit. *New Phytologist*, 226, 1550–1566.

Haldimann, P. & Feller, U. (2005) Growth at moderately elevated temperature alters the physiological response of the photosynthetic apparatus to heat stress in pea (*Pisum sativum* L.) leaves. *Plant, Cell & Environment*, 28, 302–317.

Hall, M., Medlyn, B.E., Abramowitz, G., Franklin, O., Rantfors, M. & Linder, S. et al. (2013) Which are the most important parameters for modelling carbon assimilation in boreal Norway spruce under elevated [CO_2] and temperature conditions? *Tree Physiology*, 33, 1156–1176.

Hara, C., Inoue, S., Ishii, H.R., Okabe, M., Nakagaki, M. & Kobayashi, H. (2021) Tolerance and acclimation of photosynthesis of nine urban tree species to warmer growing conditions. *Trees*, 35, 1793–1806.

Hernández, G.G., Winter, K. & Slot, M. (2020) Similar temperature dependence of photosynthetic parameters in sun and shade leaves of three tropical tree species. *Tree Physiology*, 40, 637–651.

Hew, C.-S., Krotkov, G. & Canvin, D.T. (1969) Effects of temperature on photosynthesis and CO_2 evolution in light and darkness by Green leaves. *Plant Physiology*, 44, 671–677.

Hikosaka, K., Ishikawa, K., Borjigidai, A., Muller, O. & Onoda, Y. (2005) Temperature acclimation of photosynthesis: mechanisms involved in the changes in temperature dependence of photosynthetic rate. *Journal of Experimental Botany*, 57, 291–302.

HilleRisLambers, J., Ettinger, A.K., Ford, K.R., Haak, D.C., Horwith, M., Miner, B.E. et al. (2013) Accidental experiments: ecological and evolutionary insights and opportunities derived from global change. *Oikos*, 122, 1649–1661.

IPCC. (2021) Climate change 2021: the physical science basis. In: Masson-Delmotte, V., Zhai, P., Pirani, A., Connors, S. & Péan, C. et al. (Eds.) *Contribution of Working Group I to the Sixth Assessment Report of the Intergovernmental Panel on Climate Change*. IPCC.

Jeevalakshmi, D., Reddy, S.N. & Manikiam, B. (2017) Land surface temperature retrieval from LANDSAT data using emissivity estimation. *International Journal of Applied Engineering Research*, 12, 9679–9687.

Juárez-López, F.J., Escudero, A. & Mediavilla, S.J.T.P (2008) Ontogenetic changes in stomatal and biochemical limitations to photosynthesis of two co-occurring Mediterranean oaks differing in leaf life span. *Tree Physiology*, 28, 367–374.

June, T., Evans, J.R. & Farquhar, G.D. (2004) A simple new equation for the reversible temperature dependence of photosynthetic electron transport: a study on soybean leaf. *Functional Plant Biology*, 31(3), 275–283.

Kattge, J. & Knorr, W. (2007) Temperature acclimation in a biochemical model of photosynthesis: a reanalysis of data from 36 species. *Plant, Cell & Environment*, 30, 1176–1190.

Knoerr, K.R. & Gay, L.W. (1965) Tree leaf energy balance. *Ecology*, 46, 17–24.

Kullberg, A.T. & Feeley, K.J. (2022) Limited acclimation of leaf traits and leaf temperatures in a subtropical urban heat island. *Tree Physiology*, 42, 2266–2281.

Kumarathunge, D.P., Medlyn, B.E., Drake, J.E., Tjoelker, M.G., Aspinwall, M.J., Battaglia, M. et al. (2019) Acclimation and adaptation components of the temperature dependence of plant photosynthesis at the global scale. *New Phytologist*, 222, 768–784.

Kuznetsova, A., Brockhoff, P.B. & Christensen, R.H.B. (2017) lmerTest package: tests in linear mixed effects models. *Journal of Statistical Software*, 82, 1–26.

Landsat Missions. *Using the USGS landsat level-1 data product*. USGS. https://www.usgs.gov/landsat-missions/using-usgs-landsat-level-1-data-product

Lin, Y.-S., Medlyn, B.E. & Ellsworth, D.S. (2012) Temperature responses of leaf net photosynthesis: the role of component processes. *Tree Physiology*, 32, 219–231.

Lin, Y.-S., Medlyn, B.E., De Kauwe, M.G. & Ellsworth, D.S. (2013) Biochemical photosynthetic responses to temperature: how do interspecific differences compare with seasonal shifts? *Tree Physiology*, 33, 793–806.

Lombardozzi, D.L., Bonan, G.B., Smith, N.G., Dukes, J.S. & Fisher, R.A. (2015) Temperature acclimation of photosynthesis and respiration: a key uncertainty in the carbon cycle-climate feedback. *Geophysical Research Letters*, 42, 8624–8631.

Lumley, T. (2004) The leaps package. R Project for Statistical Computing.

Medlyn, B.E., Dreyer, E., Ellsworth, D., Forstreuter, M., Harley, P.C., Kirschbaum, M.U.F. et al. (2002) Temperature response of parameters of a biochemically based model of photosynthesis. II. A review of experimental data. *Plant, Cell & Environment*, 25, 1167–1179.

Meineke, E., Youngsteadt, E., Dunn, R.R. & Frank, S.D. (2016) Urban warming reduces aboveground carbon storage. *Proceedings of the Royal Society B: Biological Sciences*, 283, 20161574.

Meinzer, F.C., Smith, D.D., Woodruff, D.R., Marias, D.E., McCulloh, K.A. & Howard, A.R. et al. (2017) Stomatal kinetics and photosynthetic gas

exchange along a continuum of isohydric to anisohydric regulation of plant water status. *Plant, Cell & Environment*, 40, 1618–1628.

Mercado, L.M., Medlyn, B.E., Huntingford, C., Oliver, R.J., Clark, D.B., Sitch, S. et al. (2018) Large sensitivity in land carbon storage due to geographical and temporal variation in the thermal response of photosynthetic capacity. *New Phytologist*, 218, 1462–1477.

Mooney, H.A., Björkman, O. & Collatz, G.J. (1978) Photosynthetic acclimation to temperature in the desert shrub, *Larrea divaricata*: I. Carbon dioxide exchange characteristics of intact leaves. *Plant Physiology*, 61, 406–410.

Onoda, Y. (2005) Seasonal change in the balance between capacities of RuBP carboxylation and RuBP regeneration affects CO_2 response of photosynthesis in *Polygonum cuspidatum*. *Journal of Experimental Botany*, 56, 755–763.

Peak, D. & Mott, K.A. (2011) A new, vapour-phase mechanism for stomatal responses to humidity and temperature. *Plant, Cell & Environment*, 34, 162–178.

Pearcy, R.W. (1977) Acclimation of photosynthetic and respiratory carbon dioxide exchange to growth temperature in *Atriplex lentiformis* (Torr.) Wats. *Plant Physiology*, 59, 795–799.

Perez, T.M., Socha, A., Tserej, O. & Feeley, K.J. (2021) Photosystem II heat tolerances characterize thermal generalists and the upper limit of carbon assimilation. *Plant, Cell, & Environment*, 44, 2321–2330.

Reynolds-Henne, C.E., Langenegger, A., Mani, J., Schenk, N., Zumsteg, A. & Feller, U. (2010) Interactions between temperature, drought and stomatal opening in legumes. *Environmental and Experimental Botany*, 68, 37–43.

Rogers, A., Medlyn, B.E., Dukes, J.S., Bonan, G., Caemmerer, S., Dietze, M.C. et al. (2017) A roadmap for improving the representation of photosynthesis in Earth system models. *New Phytologist*, 213, 22–42.

Rowland, L., Harper, A., Christoffersen, B.O., Galbraith, D.R., Imbuzeiro, H.M.A., Powell, T.L. et al. (2015) Modelling climate change responses in tropical forests: similar productivity estimates across five models, but different mechanisms and responses. *Geoscientific Model Development*. 8, 1097–1110.

Sage, R.F. & Kubien, D.S. (2007) The temperature response of C_3 and C_4 photosynthesis. *Plant, Cell & Environment*, 30, 1086–1106.

Sage, R.F., Way, D.A. and Kubien, D.S. (2008) Rubisco, Rubisco activase, and global climate change. *Journal of Experimental Botany*, 59, 1581–1595.

Säll, T. & Pettersson, P. (1994) A model of photosynthetic acclimation as a special case of reaction norms. *Journal of Theoretical Biology*, 166, 1–8.

Salvucci, M.E. & Crafts-Brandner, S.J. (2004) Inhibition of photosynthesis by heat stress: the activation state of Rubisco as a limiting factor in photosynthesis. *Physiologia Plantarum*, 120, 179–186.

Santiago, L.S. & Mulkey, S.S. (2003) A test of gas exchange measurements on excised canopy branches of ten tropical tree species. *Photosynthetica*, 41, 343–347.

Scafaro, A.P., Xiang, S., Long, B.M., Bahar, N.H.A., Weerasinghe, L.K., Creek, D. et al. (2017) Strong thermal acclimation of photosynthesis in tropical and temperate wet-forest tree species: the importance of altered Rubisco content. *Global Change Biology*, 23, 2783–2800.

Sendall, K.M., Reich, P.B., Zhao, C., Jihua, H., Wei, X., Stefanski, A. et al. (2015) Acclimation of photosynthetic temperature optima of temperate and boreal tree species in response to experimental forest warming. *Global Change Biology*, 21, 1342–1357.

Silim, S.N., Ryan, N. & Kubien, D.S. (2010) Temperature responses of photosynthesis and respiration in *Populus balsamifera* L.: acclimation versus adaptation. *Photosynthesis Research*, 104, 19–30.

Slot, M., Rifai, S.W. & Winter, K. (2021) Photosynthetic plasticity of a tropical tree species, *Tabebuia rosea*, in response to elevated temperature and [CO_2]. *Plant, Cell & Environment*, 77, 2347–2364.

Slot, M. & Winter, K. (2016) The effects of rising temperature on the ecophysiology of tropical forest trees. In: Goldstein, G & Santiago, L. S. (Eds.) *Tropical tree physiology Vol. 6*. Springer, pp. 385–412.

Slot, M. & Winter, K. (2017a) In situ temperature relationships of biochemical and stomatal controls of photosynthesis in four lowland tropical tree species. *Plant, Cell & Environment*, 40, 3055–3068.

Slot, M. & Winter, K. (2017b) In situ temperature response of photosynthesis of 42 tree and liana species in the canopy of two Panamanian lowland tropical forests with contrasting rainfall regimes. *New Phytologist*, 214, 1103–1117.

Slot, M. & Winter, K. (2017c) Photosynthetic acclimation to warming in tropical forest tree seedlings. *Journal of Experimental Botany*, 68, 2275–2284.

Slot, M. & Winter, K. (2018) High tolerance of tropical sapling growth and gas exchange to moderate warming. *Functional Ecology*, 32, 599–611.

Smith, M.N., Taylor, T.C., van Haren, J., Rosolem, R., Restrepo-Coupe, N., Adams, J. et al. (2020) Empirical evidence for resilience of tropical forest photosynthesis in a warmer world. *Nature Plants*, 6, 1225–1230.

Smith, N.G. & Dukes, J.S. (2013) Plant respiration and photosynthesis in global-scale models: incorporating acclimation to temperature and CO_2. *Global Change Biology*, 19, 45–63.

Smith, N.G. & Keenan, T.F. (2020) Mechanisms underlying leaf photosynthetic acclimation to warming and elevated CO_2 as inferred from least-cost optimality theory. *Global Change Biology*, 26, 5202–5216.

Sperlich, D., Chang, C.T., Peñuelas, J. & Sabaté, S. (2019) Responses of photosynthesis and component processes to drought and temperature stress: are Mediterranean trees fit for climate change? *Tree Physiology*, 39, 1783–1805.

Stefanski, A., Bermudez, R., Sendall, K.M., Montgomery, R.A. & Reich, P.B. (2020) Surprising lack of sensitivity of biochemical limitation of photosynthesis of nine tree species to open-air experimental warming and reduced rainfall in a southern boreal forest. *Global Change Biology*, 26, 746–759.

Tan, Z.-H., Zeng, J., Zhang, Y.-J., Slot, M., Gamo, M., Hirano, T. et al. (2017) Optimum air temperature for tropical forest photosynthesis: mechanisms involved and implications for climate warming. *Environmental Research Letters*, 12, 054022.

Urban, J., Ingwers, M.W., McGuire, M.A. & Teskey, R.O. (2017) Increase in leaf temperature opens stomata and decouples net photosynthesis from stomatal conductance in *Pinus taeda* and *Populus deltoides* x nigra. *Journal of Experimental Botany*, 68, 1757–1767.

Vårhammar, A., Wallin, G., McLean, C.M., Dusenge, M.E., Medlyn, B.E., Hasper, T.B. et al. (2015) Photosynthetic temperature responses of tree species in Rwanda: evidence of pronounced negative effects of high temperature in montane rainforest climax species. *New Phytologist*, 206, 1000–12.

Verryckt, L.T., Van Langenhove, L., Ciais, P., Courtois, E.A., Vicca, S., Peñuelas, J. et al. (2020) Coping with branch excision when measuring leaf net photosynthetic rates in a lowland tropical forest. *Biotropica*, 52, 608–615.

Way, D.A. & Sage, R.F. (2008) Thermal acclimation of photosynthesis in black spruce [*Picea mariana* (Mill.) B.S.P.]. *Plant, Cell & Environment*, 31, 1250–1262.

Way, D.A. & Yamori, W. (2014) Thermal acclimation of photosynthesis: on the importance of adjusting our definitions and accounting for thermal acclimation of respiration. *Photosynthesis Research*, 119, 89–100.

Wong, S.C., Cowan, I.R. & Farquhar, G.D. (1979) Stomatal conductance correlates with photosynthetic capacity. *Nature*, 282, 424–426.

Wood, S. (2017) Package "mgcv": mixed GAM computation vehicle with GCV/AIC/REML smoothness estimation. R Package Version.

Wright, I.J., Dong, N., Maire, V., Prentice, I.C., Westoby, M., Díaz, S. et al. (2017) Global climatic drivers of leaf size. *Science*, 357, 917–921.

Yamaguchi, D.P., Nakaji, T., Hiura, T. & Hikosaka, K. (2016) Effects of seasonal change and experimental warming on the temperature dependence of photosynthesis in the canopy leaves of *Quercus serrata*. *Tree Physiology*, 36, 1283–1295.

Yamori, W., Suzuki, K., Noguchi, K., Nakai, M. & Terashima, I. (2006) Effects of Rubisco kinetics and Rubisco activation state on the temperature dependence of the photosynthetic rate in spinach leaves from contrasting growth temperatures. *Plant, Cell & Environment*, 29, 1659–1670.

Youngsteadt, E., Dale, A.G., Terando, A.J., Dunn, R.R. & Frank, S.D. (2015) Do cities simulate climate change? A comparison of herbivore response to urban and global warming. *Global Change Biology*, 21, 97–105.

SUPPORTING INFORMATION

Additional supporting information can be found online in the Supporting Information section at the end of this article.

How to cite this article: Kullberg, A.T., Slot, M. & Feeley, K.J. (2023) Thermal optimum of photosynthesis is controlled by stomatal conductance and does not acclimate across an urban thermal gradient in six subtropical tree species. *Plant, Cell & Environment*, 1–19. https://doi.org/10.1111/pce.14533